

### 3. ผลการวิจัยและวิจารณ์ผลการทดลอง (Results and Discussions)



#### 3.1 Characterization of metal nanoparticles

The metal nanoparticles were characterized by UV-Vis spectrophotometer and Transmission Electron Microscopy (TEM). A typical absorption spectrum of metal nanoparticles was shown in Figure 3.1 . The plasmon wavelength maxima ( $\lambda_{\max}$ ) indicate the size of metal nanoparticles. The  $\lambda_{\max}$  of gold and silver nanoparticles used in this research are approximately at 520 nm and 400 nm, respectively.

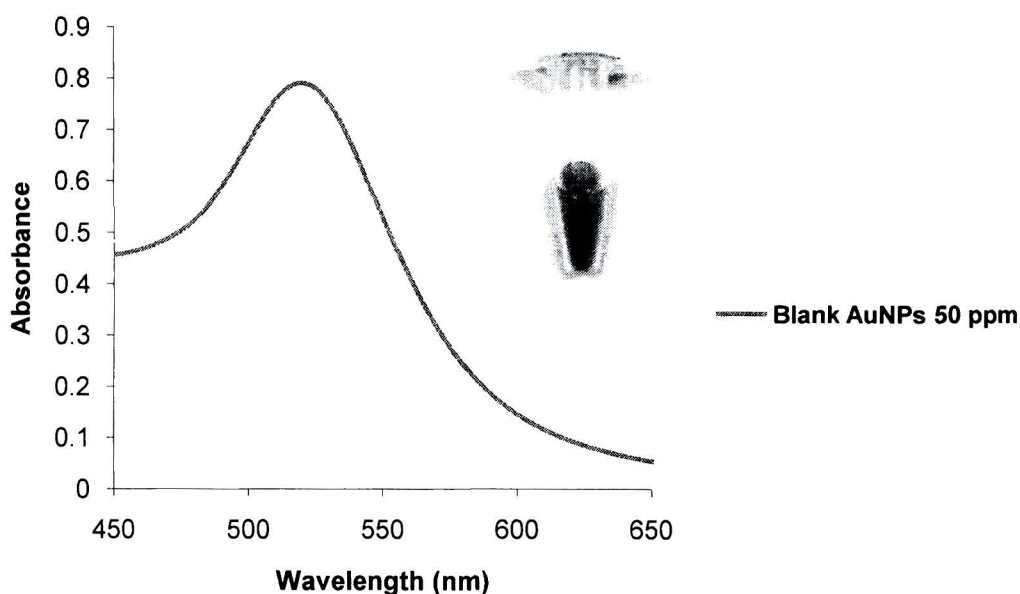
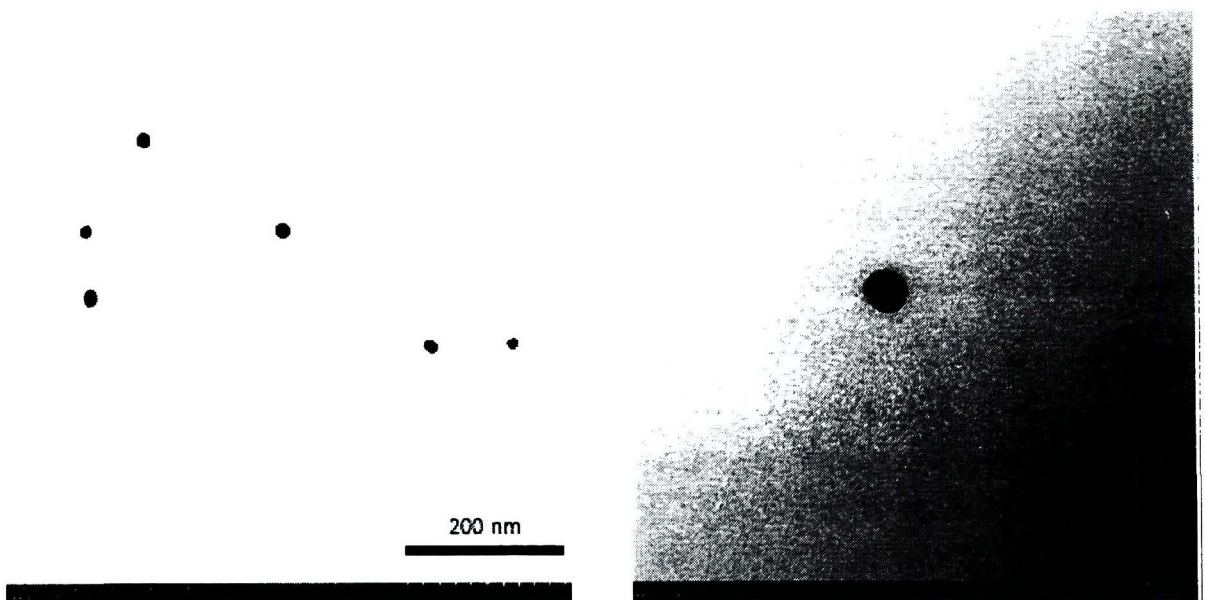


Figure 3.1 The characterization of AuNPs using spectrophotometer

These values of citrate-stabilized gold nanoparticles are similar with other different synthetic methods, reviewed by Daniel (25). The red shift in  $\lambda_{\max}$  is associated with an increase in the mean size of the gold nanoparticles or modification in the surrounding media. Moreover,

any change in  $\Delta\lambda$  indicates an aggregation of gold nanoparticles or modification in the surrounding media. The size and size distribution of metal nanoparticles are shown in Figure 3.1.

Further characterization of gold nanoparticles, a Transmission Electron Microscope (TEM) was used for determining the size and size distribution of citrate-stabilized gold nanoparticles. The size and size distribution of citrate-stabilized gold nanoparticles are shown in Figure 3.2. TEM images show that the diameter of spherical gold nanoparticles range from 10 to 15 nm with monodisperse size distribution.



**Figure 3.2** The characterization of metal nanoparticles using TEM. (A) Shows a spherical gold nanoparticles with diameter around  $\approx 15$  nm.

The size and shape of synthesized gold nanoparticles are similar to the citrate reduction of  $\text{HAuCl}_4$  in water, which was introduced by Turkevitch (26). This method leads to 10-20 nm spherical gold nanoparticles with monodisperse size distribution.

The AuNPs were further tested by using zeta potential and zeta sizer instrument. The results are shown as below. 3.3 is value of zeta potential of gold nanoparticles. The result of zeta potential shows that the surface of gold nanoparticles has negative potential and the value is

equal to -44 mV. Figure 3.4 illustrates size distribution of gold nanoparticles colloid; average size of nanoparticles is equal to 15 nm in diameter.

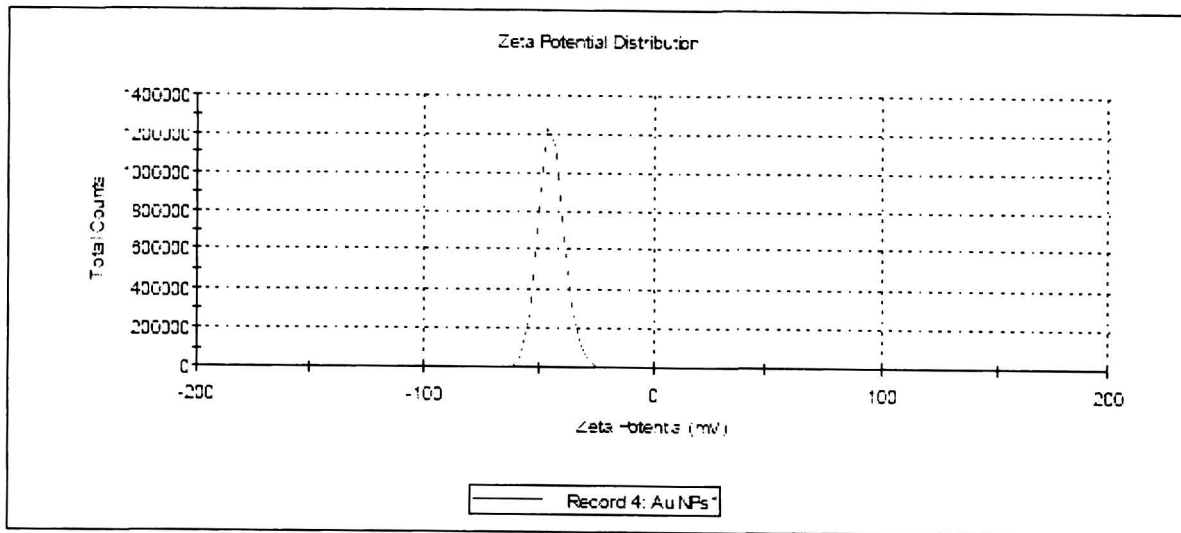


Figure 3.3 – Zeta potential of gold nanoparticles is measured by nanosizer. Zeta potential is around -44 mV.

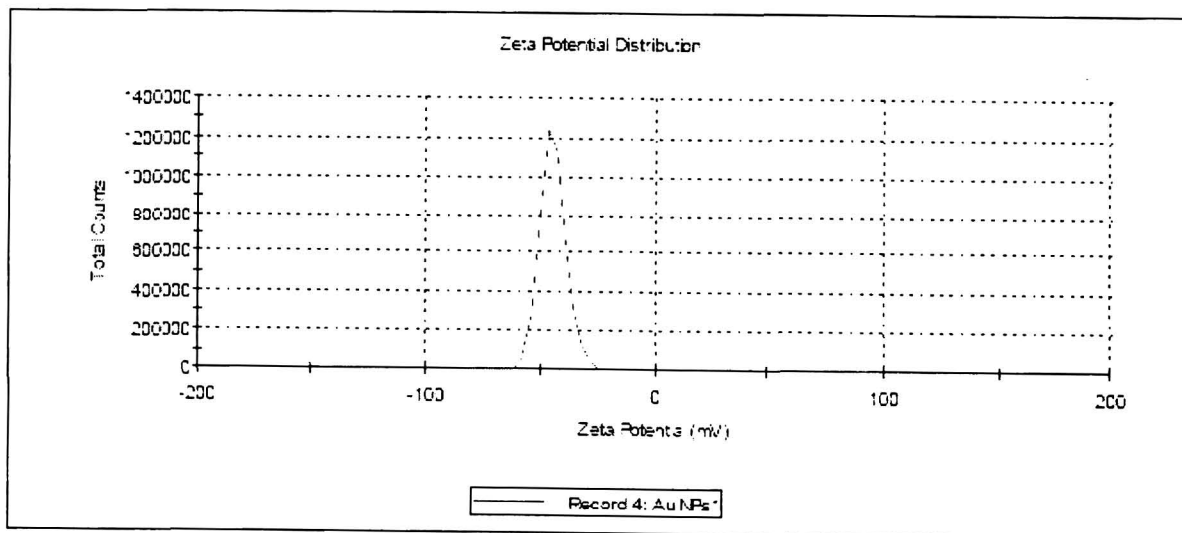


Figure 3.4 - Size distribution of gold nanoparticles is characterized by nanosizer. Maximum peak is about 15 nm in diameter

Citrate reduction has been found to be a very suitable method for gold nanoparticles synthesis. In this project, the synthesized gold nanoparticles have uniformly spherical shape. From TEM image, size of the nanoparticles is approximately 15 nm in diameter which is

confirmed again by result from nanosizer. This size and shape of gold nanoparticles are comparable to previous experiment from Kumar *et al* (2008) and it is appropriate to be used as sensing materials. For zeta potential of gold nanoparticles which is -44 mV, this negative potential is result of negative charge from citrate which is acting as stabilizer around the nanoparticles. From zeta potential result, it can refer that gold nanoparticles inside will has partial positive charge which is a proper potential for electrostatic conjugation of antibody onto gold nanoparticles.

### **3.2 Effects of gold nanoparticles on cell morphology**

The cell morphology of HeLa cells in the presence of gold nanoparticles was investigated using Light Microscope (LM). After incubation of gold nanoparticles with various concentrations of citrate-stabilized gold nanoparticles, cell morphology of HeLa cells was observed and photographs were taken. Cell morphology of HeLa cells in gold nanoparticles treated groups was compared with negative and positive control groups, as shown in figure 3.5 and 3.6. In negative control groups, HeLa cells were cultured in the media for 1, 2 and 3 days, whereas positive control groups, HeLa cells were incubated with DMSO.

In the negative control, cells were able to continuously grow until the third day with increasing cell proliferation. The HeLa cells morphology is well spread and attach on the plate, as shown in figure 3.5.

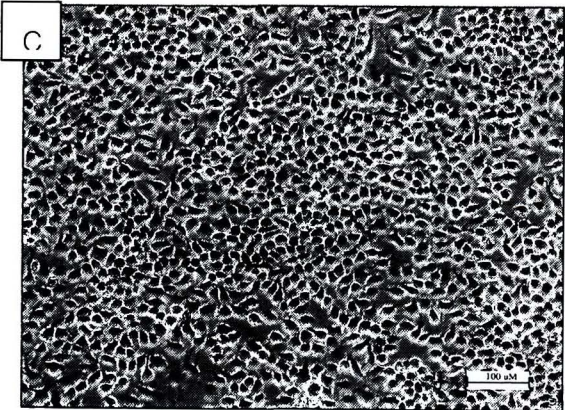
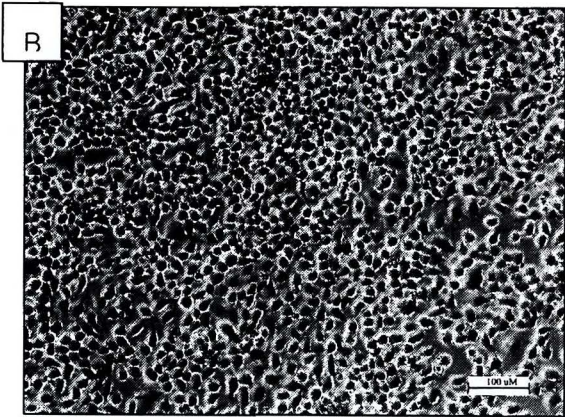
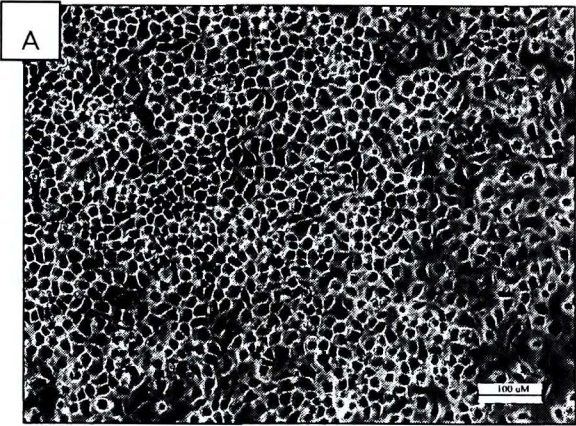


Figure 3.5 General cell morphology in negative control. The cultivation of HeLa cells alone for 1, 2 and 3 days (A-C).

HeLa cells morphology in positive groups is shown in figure 3.6. The decreasing cell proliferation and cell adhesion were obviously observed. These results indicated the characteristic of cell death.

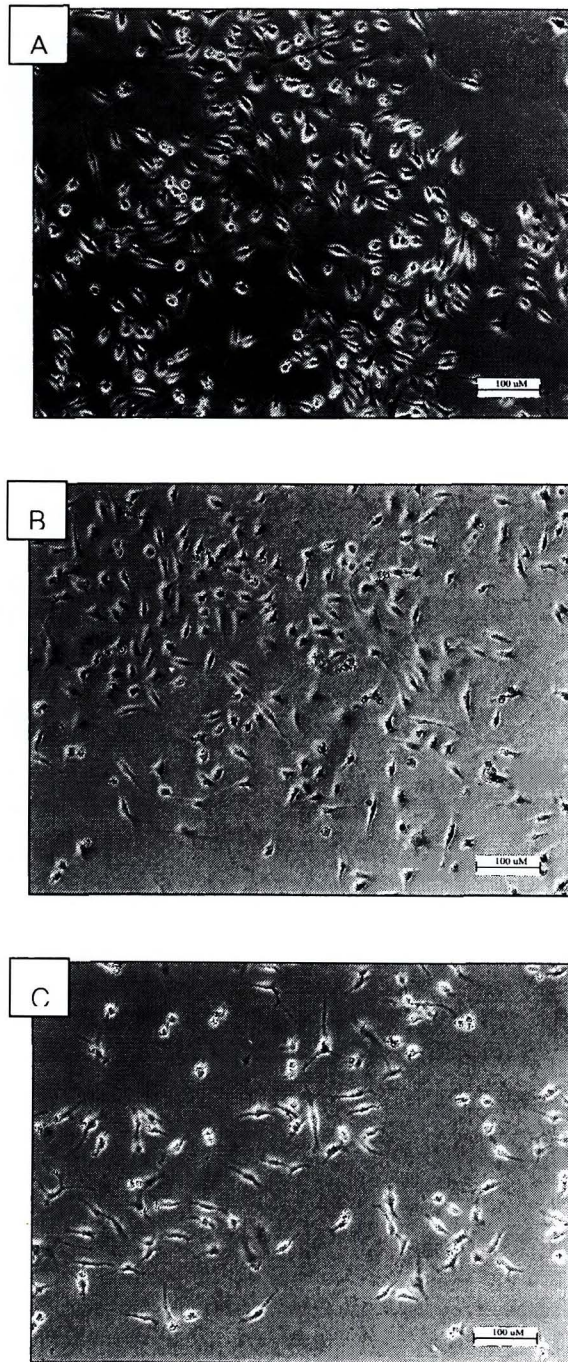


Figure 3.6 HeLa cells morphology in positive control. The incubation of HeLa cells with DMSO for 1, 2 and 3 days (A-C).

HeLa cells morphology in the presence of citrate is shown in figure 3.7, there was no distinct change in morphology could be observed.

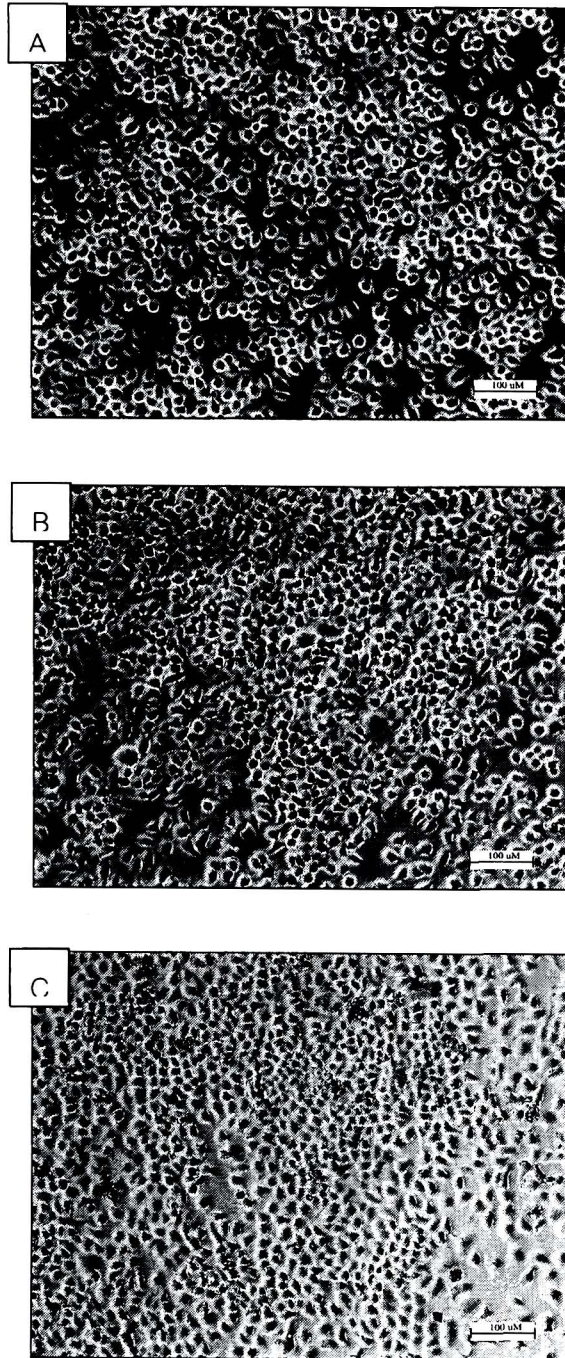


Figure 3.7 HeLa cells morphology in the presence of citrate. The incubation of HeLa cells with citrate for 1, 2 and 3 days (A-C).

HeLa cells morphology in the presence of 10 ug/mL gold nanoparticles is shown in figure 3.8, morphological changes were not observed after incubation for 1, 2 and 3 days.

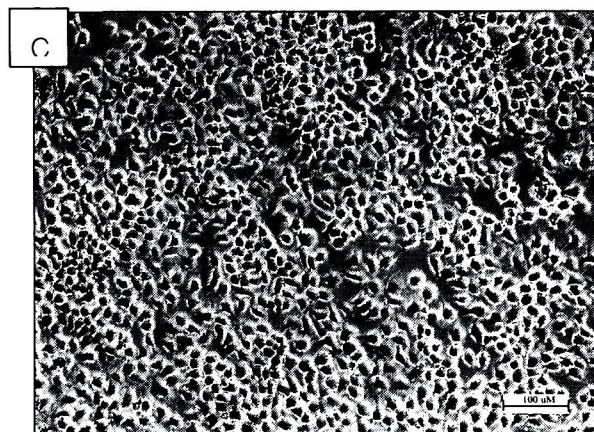
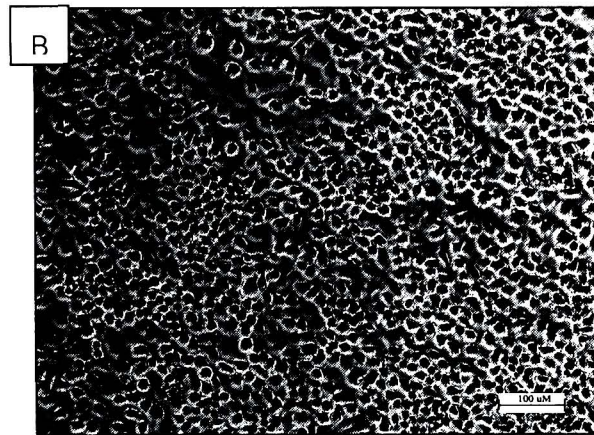
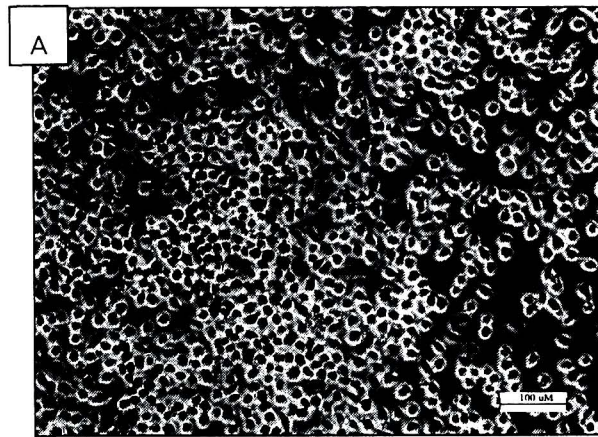


Figure 3.8 HeLa cells morphology in the presence of 10 ug/mL gold nanoparticles. The incubation of HeLa cells with 10 ug/mL gold nanoparticles for 1, 2 and 3 days (A-C).

HeLa cells morphology in the presence of 50 ug/mL gold nanoparticles is shown in figure 3.9, morphological changes were not found.

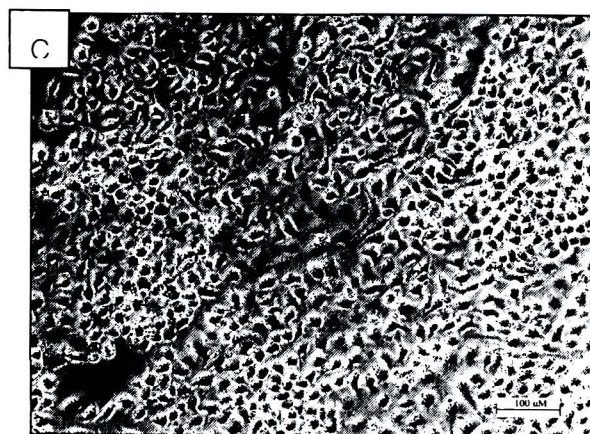
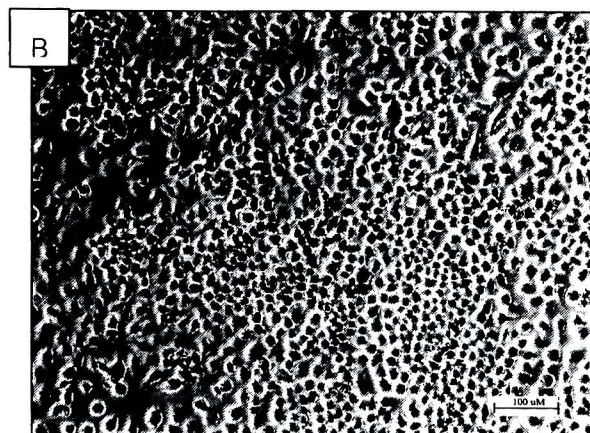
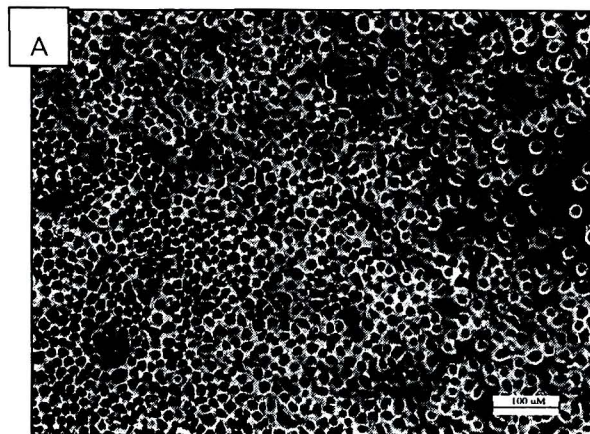
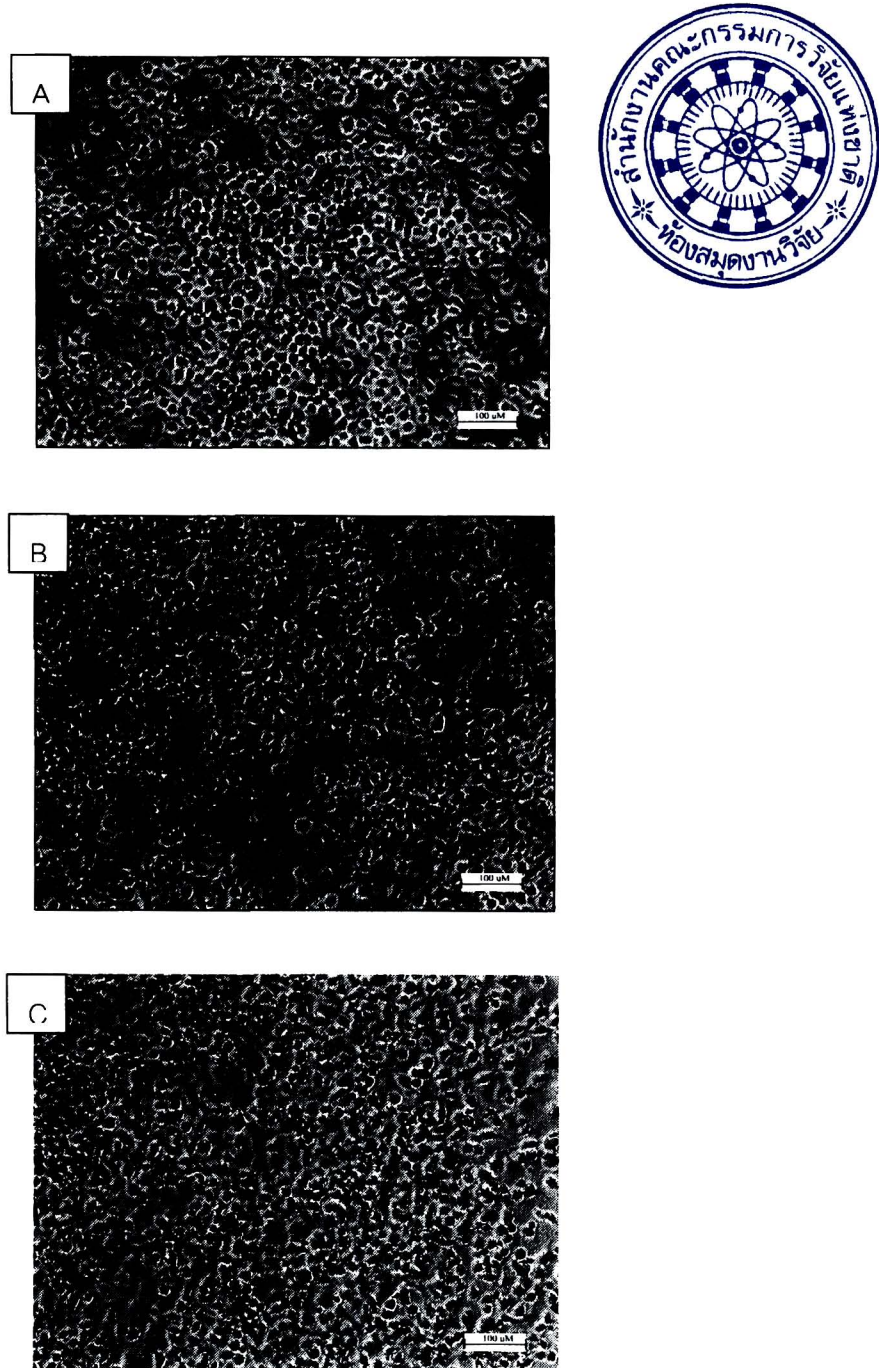


Figure 3.9 HeLa cells morphology in the presence of 50 ug/mL gold nanoparticles. The incubation of HeLa cells with 50 ug/mL gold nanoparticles for 1, 2 and 3 days (A-C).

HeLa cells morphology in the presence of 100 ug/mL gold nanoparticles is shown in figure 3.10, morphological changes were observed. The cells become shrink and irregular after third day incubation with gold nanoparticles.



**Figure 3.10 HeLa cells morphology in the exposure to 100 ug/mL gold nanoparticles.** The incubation of HeLa cells with 100 ug/mL gold nanoparticles for 1, 2 and 3 days (A-C).

These experiments show that the cells were well spread and there was no distinct change in morphology after the incubation with 10 and 50 ug/mL of gold nanoparticles relative to untreated cells. However, dramatic changes occurred with 100 ug/mL gold nanoparticles treated group in the third day. The cells become irregular, contract and detach. Thus, 100 ug/mL gold nanoparticles is considered as the toxic concentration for cells. It could be concluded that the dramatic changes induced by an increasing gold nanoparticles concentration and incubation time. This information should be considered for further in vivo application of gold nanoparticles.

These findings are in agreement with Pernodet (35) who reported the dose-dependent cytotoxicity. The contracted fibroblast cells and decreasing cell proliferation were observed. They suggested that cytoskeleton is affected in the presence of citrate-stabilized gold nanoparticles.

### **3.3 In Vitro Cytotoxicity and intra-cellular localization**

The effect of various concentrations of citrate-stabilized gold nanoparticles on HeLa cell viability was examined using MTT assay. After 1, 2 and 3 days incubation, no effect on 10 and 50 ug/mL gold nanoparticles treated groups could be observed. In contrast, the 100 ug/mL gold nanoparticles treated groups in the third day exhibited significantly toxicity. These results were compared to the control groups, as shown in figure 19. Moreover, the survival of the HeLa cells also decreased in the presence of citrate. The results show that 10 and 50 ug/mL concentration of gold nanoparticles exhibit non-toxic, except the concentrations of 100 ug/mL. It was observed that cell viability following exposure to gold nanoparticles was dependent on concentration and time incubation.

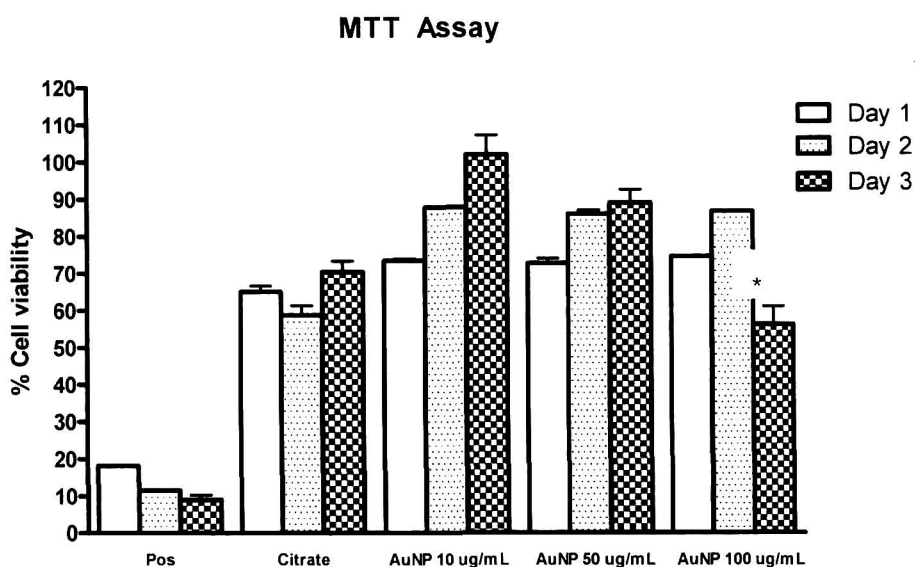
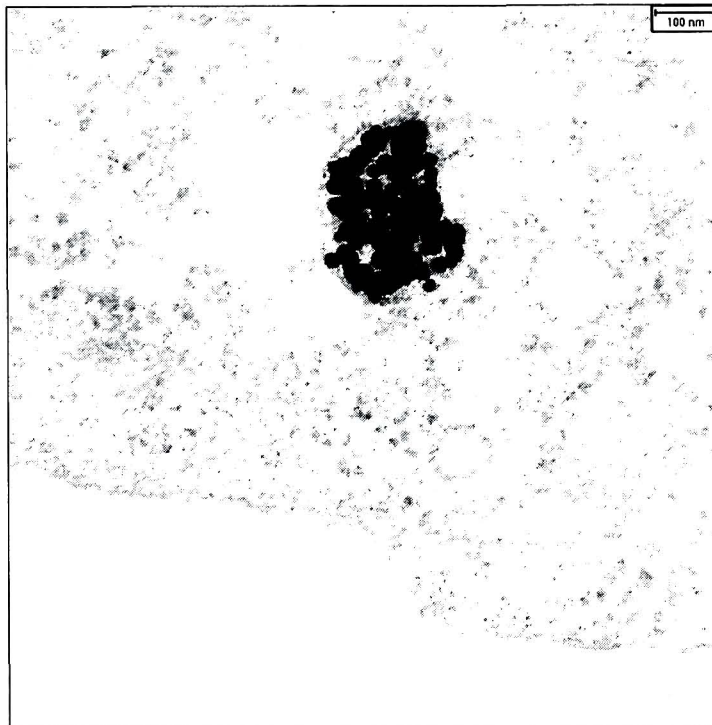


Figure 3.11 The influence of gold nanoparticles on cell viability. HeLa cells were exposed to DMSO, citrate and 10, 50, 100 ug/mL gold nanoparticles for 1, 2 and 3 days. The values reported in this graphs are the average of triplicate samples. Vertical lines denote  $\pm 1SD$  (n=3). Significant of differences between dose and time: \*, p-value<0.05).

Gold nanoparticles at the concentration of 10 and 50 ug/mL do not affect on HeLa cells, whereas 100 ug/mL gold nanoparticles exhibit cytotoxicity. These findings are in agreement with many recent previous results which reported that increasing concentration lead to increase in cytotoxicity. Our results implied that longer than 3 days incubation with 100 ug/mL gold nanoparticles can further decrease cell viability. Interestingly the HeLa cell showed greater sensitivity to 9.7 mM trisodium citrate than gold nanoparticles, which suggests that surface modification can generate cytotoxicity on HeLa cells. However, in the case of Connor(15) and Khan(16) and Tkachenko(32), they found that there are no significant differences in viability levels for gold nanoparticles at various concentrations, times and cell lines.

## Localization of gold nanoparticles

The fate and localization of gold nanoparticles were investigated using TEM. Moreover, the influence of gold nanoparticles on morphological intracellular organelles was also examined. It was found that gold nanoparticles were readily taken up by the HeLa cells and ended up in the endosome, as shown in Figure 3.12.



**Figure 3.12 Cellular uptake of 10-15 nm gold nanoparticles via the endocytosis.**

Inside the cell, most of gold nanoparticles are found in the endosomes, but gold nanoparticles are also observed freely dispersed in the cytosol. In addition, gold nanoparticles were aggregated close to but not in the mitochondria or nucleus, as illustrated in Figure 3.13. The results demonstrate that gold nanoparticles are indeed in the cytosol.

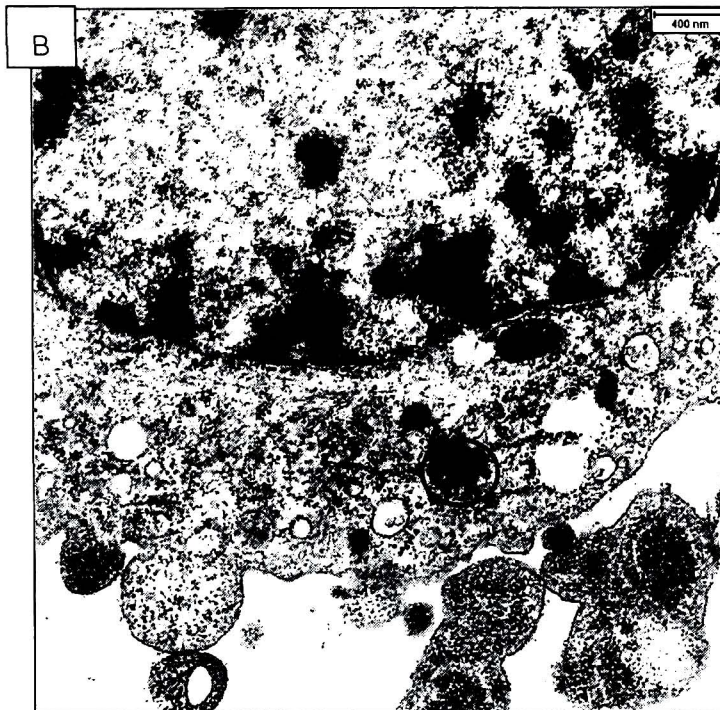
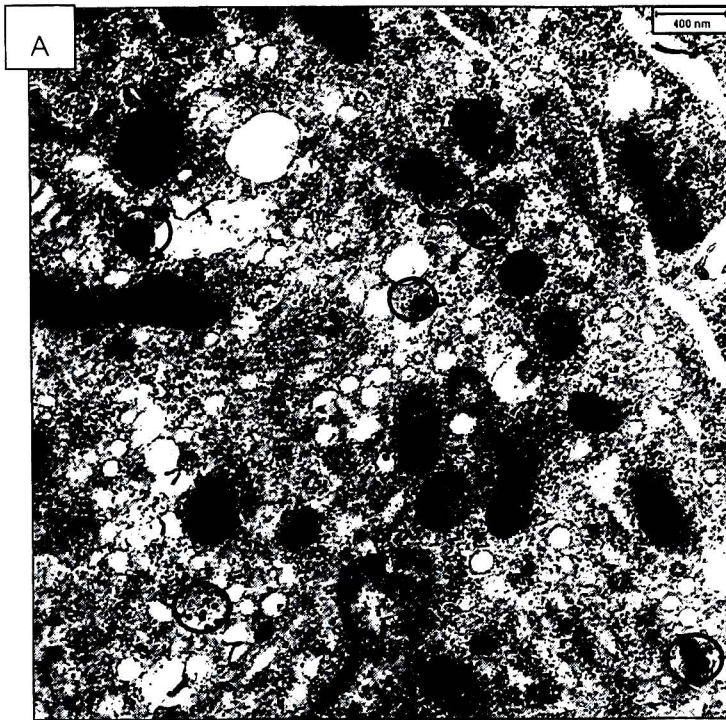
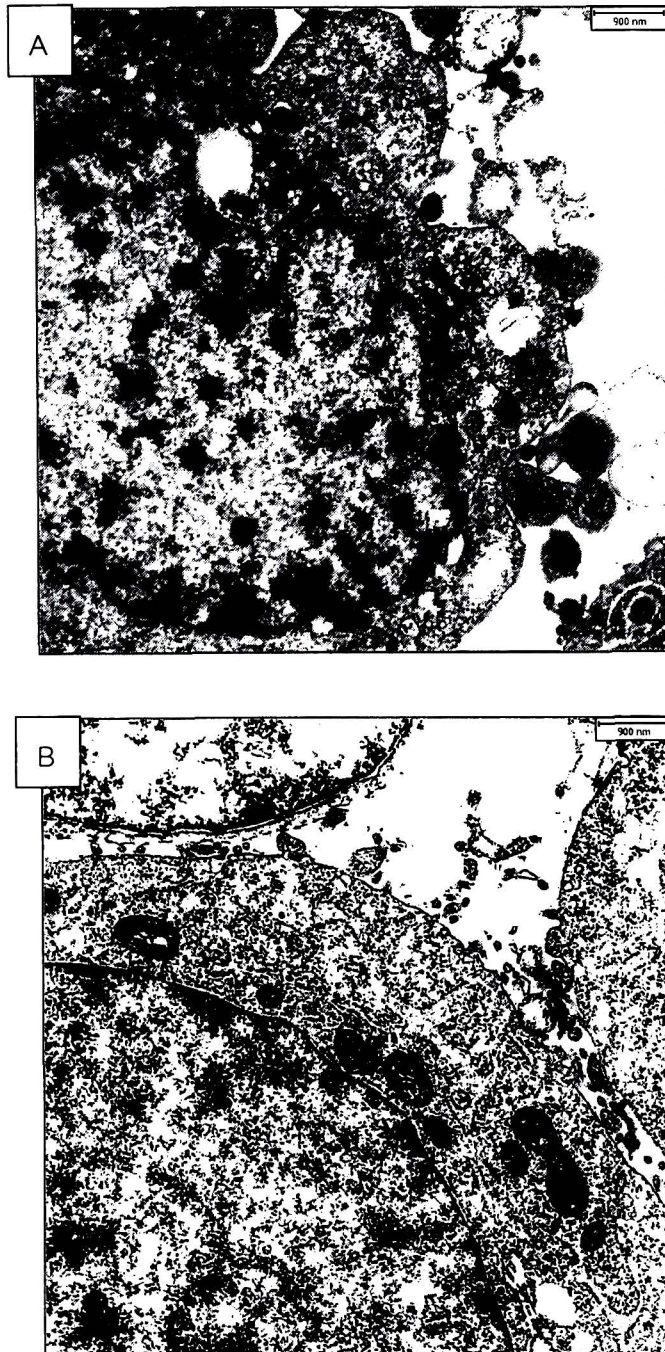


Figure 3.13 Internalization of gold nanoparticles. Fig A demonstrates that gold nanoparticles were freely dispersed in the cytosol. Fig B shows gold nanoparticles were aggregated close to but not in the mitochondria or nucleus.

The results of cells exposed to gold nanoparticles showed that nucleus, mitochondria and ER were not affected morphologically (figure 3.14).



**Figure 3.14 Intracellular organelles morphology.** Fig A shows the nuclei, mitochondria and ER were not altered in the exposure to gold nanoparticles. Fig B indicates the general morphology of intracellular organelles.

Finally, gold nanoparticles cannot penetrate nuclear membranes and attach to DNA consequently; gold nanoparticles can not cause toxicity. These findings confirm the nontoxic nature of gold nanoparticles, which enter the cells but do not affect nucleus, mitochondria and ER. Cellular uptake of gold nanoparticles is similar to previous studies. Connor *et al.* report 18 nm citrate-stabilized gold nanoparticles are taken up by K562 cells but do not cause cytotoxicity after 24 hours incubation(15). Moreover, Khan *et al.* reported 18 nm gold nanoparticles (2 nM) were trapped in vesicles and internalized inside HeLa cells after 6 hours incubation. Even after a longer incubation time, the nanoparticles did not enter the nucleus. They localized within the cytoplasm, but were not closely associated with organelles.

### 3.4 Aggregation of metal nanoparticles

#### Effect of buffer on aggregation

Due to the charge screening effect, addition of buffer or electrolyte into a solution containing metal nanoparticles resulted in a decreasing of interparticle distance and caused nanoparticles aggregation. The more electrolytes added, the more aggregation can be observed. Therefore, to make the most efficient stabilization, buffer in hybridization step should not cause aggregation of metal nanoparticles. The effect of different buffer quantity in aggregation of MNPs was shown in figure 3.15

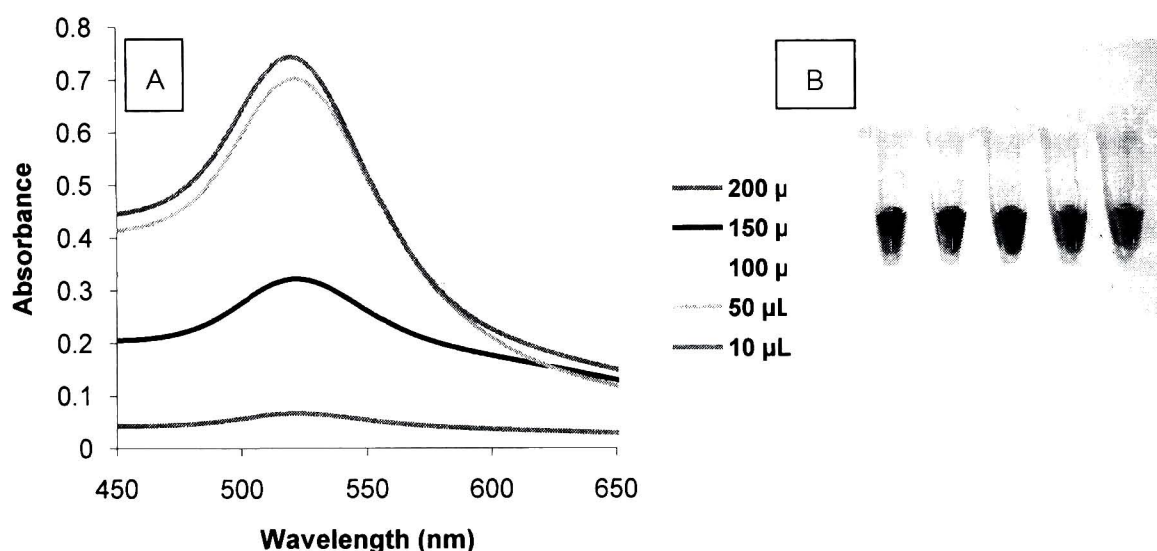


Figure 3.15 The effect of different amount of buffer to the aggregation of AuNPs. (A) UV-vis spectra of unmodified AuNPs mixing with buffer. (B) the colour changing after adding buffer, 10, 50, 100, 150 and 200  $\mu\text{L}$ , from left to right, respectively.

The decreasing in absorbance at  $\lambda_{\text{max}}$  and a concomitant red shift in the nanoparticles plasmon band indicated an aggregation of metal nanoparticles. When high amount of buffer was added into a solution of metal nanoparticles, the nanoparticles aggregated and the solution colour turned from red to blue in AuNPs solution

According to the experiment, if the buffer used in hybridization was over 100  $\mu\text{L}$ , the colour changing in aggregation can be observed with naked eye and the decreasing of absorbance at  $\lambda_{\text{max}}$  of nanoparticles can also be detected. While in 10-50  $\mu\text{L}$  of buffer, less aggregation can be observed and the colour changing of solution cannot be detected with the naked eye. Thus, the amount of buffer using in the hybridization process should not reach 50  $\mu\text{L}$ .

### Effect of salt on aggregation

The addition of NaCl into solution increased total ionic charge in solution as in the addition of buffer. Thus, the result was similar. The higher amount of salt added, the more aggregation can be observed. UV-vis spectra of mixture were shown in figure 3.16

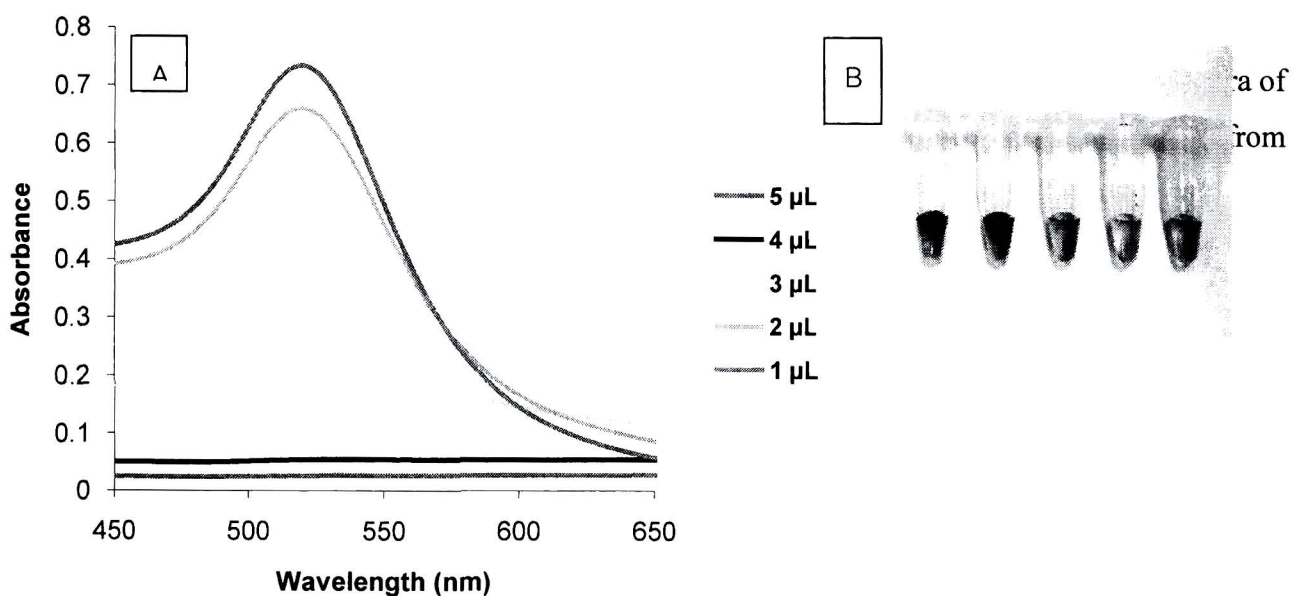


**Figure 3.16** The effect of different amount of NaCl to the aggregation of AuNPs. (A) UV-vis spectra of unmodified AuNPs mixing with NaCl. (B) the colour changing after adding 2M NaCl, 1, 2, 3, 4 and 5  $\mu\text{L}$ , from left to right, respectively

UV-vis spectra showed that aggregation, which was caused by charge screening effects, suppressed the absorption intensity. This is a slow process and the size of nanoparticle gradually growing bigger. The small red shift of the  $\lambda_{\text{max}}$  indicated that the size of nanoparticles

was slightly increased. Moreover the band width of absorption was barely changed. This indicated that size distribution remained constant.

The minimum amount of salt that caused significant changing of absorption spectra was about 3-4  $\mu\text{L}$ . The following experiments used this optimum volume of salt solution.

### Effect of DNA on aggregation

Metal nanoparticles in solution are typically stabilized by adsorbed negative ions (e.g. citrate ion) or molecule containing lone pair electron which cause negative charge on the surface. Repulsion from negative charge prevents van der Waals attraction among metal nanoparticles and thus prevents aggregation. Although the ssDNA has negative charges on the backbone causing electrostatic repulsion to the nanoparticles surface, the ssDNA is flexible and partially uncoil its structure. Under these conditions, the negative charge on the backbone is able to avert from metal nanoparticles to avoid repulsion. On the other hand, attractive van der Waals forces between the bases of ssDNA and the metal nanoparticles causes stronger ssDNA to metal interaction. The effect of DNA on AuNPs aggregation was shown in figure 3.17 (mixture1) and 3.18 (mixture2).

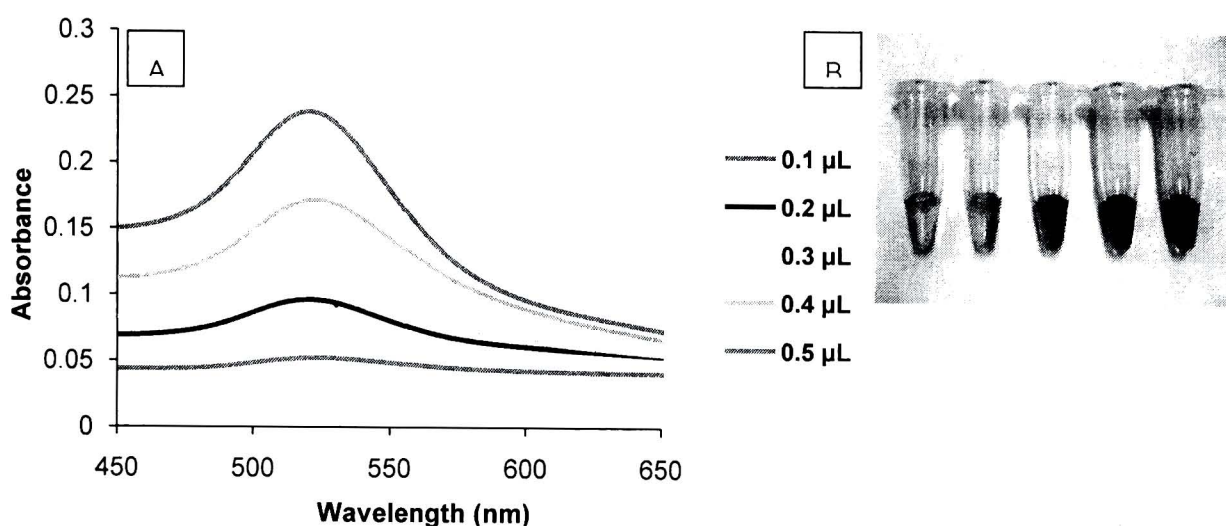


**Figure 3.17** The effect of different amount of mixture1 to the aggregation of AuNPs. (A) UV-vis spectra of unmodified AuNPs stabilized by mixture1 after mixing with NaCl. (B) the colour changing of AuNPs solution stabilized by 0.1, 0.2, 0.3, 0.4 and 0.5  $\mu\text{L}$  mixture1, from left to right, respectively.

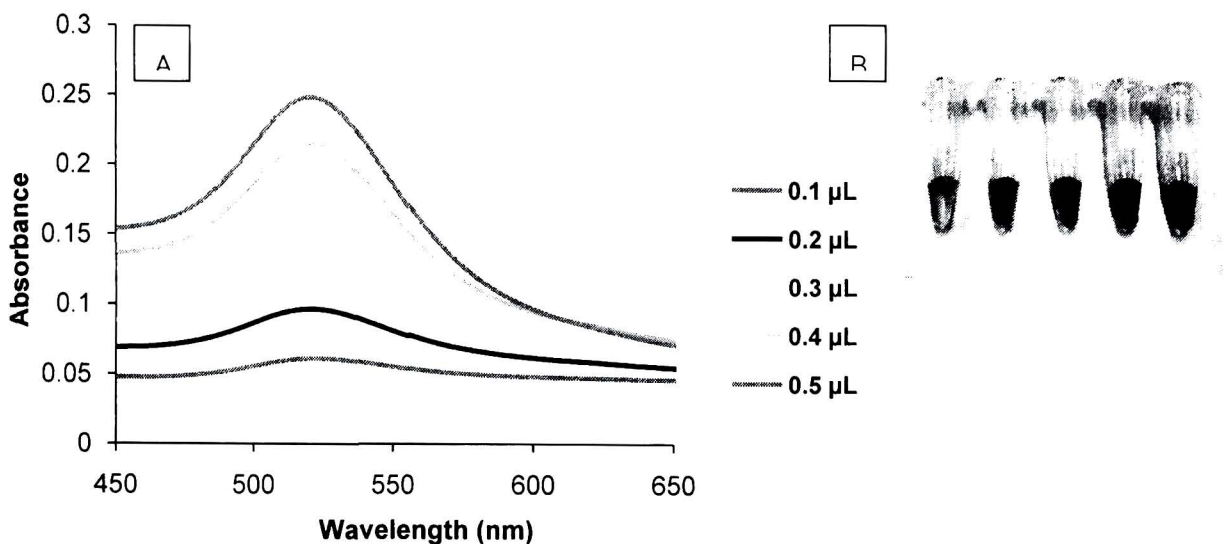


**Figure 3.18** The effect of different amount of mixture2 to the aggregation of AuNPs. (A) UV-vis spectra of unmodified AuNPs stabilized by mixture2 after mixing with NaCl. (B) the colour changing of AuNPs solution stabilized by 0.1, 0.2, 0.3, 0.4 and 0.5  $\mu\text{L}$  mixture2, from left to right, respectively.

According to the experiment, at an equal amount of mixture1 and mixture2 used to stabilize metal nanoparticles, the measured absorption intensity values were varied. The absorbance of MNPs/mixture2 mixture was higher than that of MNPs/mixture1 mixture. It indicated that the metal nanoparticles stabilization efficiency of mixture2 is higher than mixture1. Since mixture2 sequence contain more adenine base. Among four nucleobases, Adenine exhibits stronger base stacking due to its high aromaticity. Thus it promoted uncoil of DNA and caused adsorption faster and more efficiently than mixture1.

Although the colour of solution was depended on the amount of ssDNA, the addition of excess ssDNA cannot improve stability because the limited amount of nanosurface. As in AgNPs aggregation, more than 2  $\mu\text{L}$  of DNA was over excess and causes insignificantly changing in colour of solution. On the other hand, solutions with only a few ssDNA had distinctly different in absorption spectra and colloid colour.

In contrast, dsDNA has different electrostatic properties due to the double-helix geometry that always turn the negatively charged phosphate backbone out. Therefore, repulsion between the charged phosphate backbone of dsDNA and the negative charge of stabilizer

dominated the electrostatic interaction between the metal nanoparticles and dsDNA. As a consequence, dsDNA is not adsorbed onto the nanoparticles surface. The result of dsDNA stabilized metal nanoparticles was shown in figure 3.19

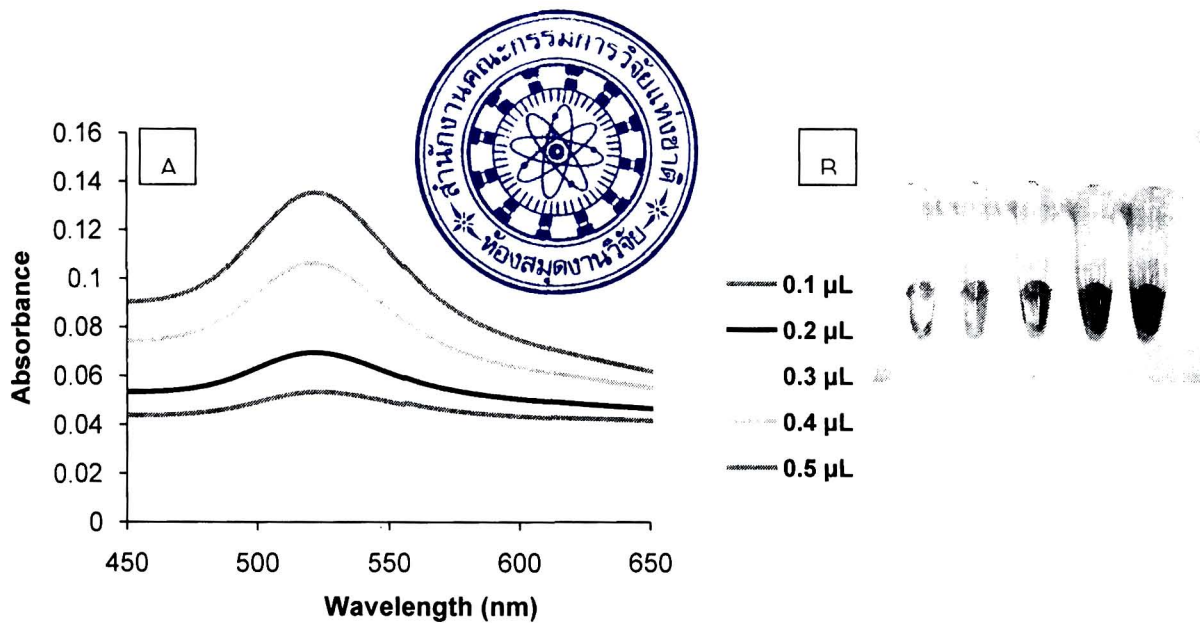


**Figure 3.19** The effect of different amount of mixture3 to the aggregation of AuNPs. (A) UV-vis spectra of unmodified AuNPs stabilized by mixture3 after mixing with NaCl. (B) the colour changing of AuNPs solution stabilized by 0.1, 0.2, 0.3, 0.4 and 0.5  $\mu\text{L}$  mixture3, from left to right, respectively.

With the increasing of mixture3, absorbance intensity was also increased though dsDNA cannot stabilize the MNPs, because hybridization was a reversible process and some of ssDNA still remained which able to stabilize metal nanoparticles.

The Experiment condition that make the aggregation of metal nanoparticles stabilized by mixture1-3 clearly detected with naked eye was shown in figure 3.20

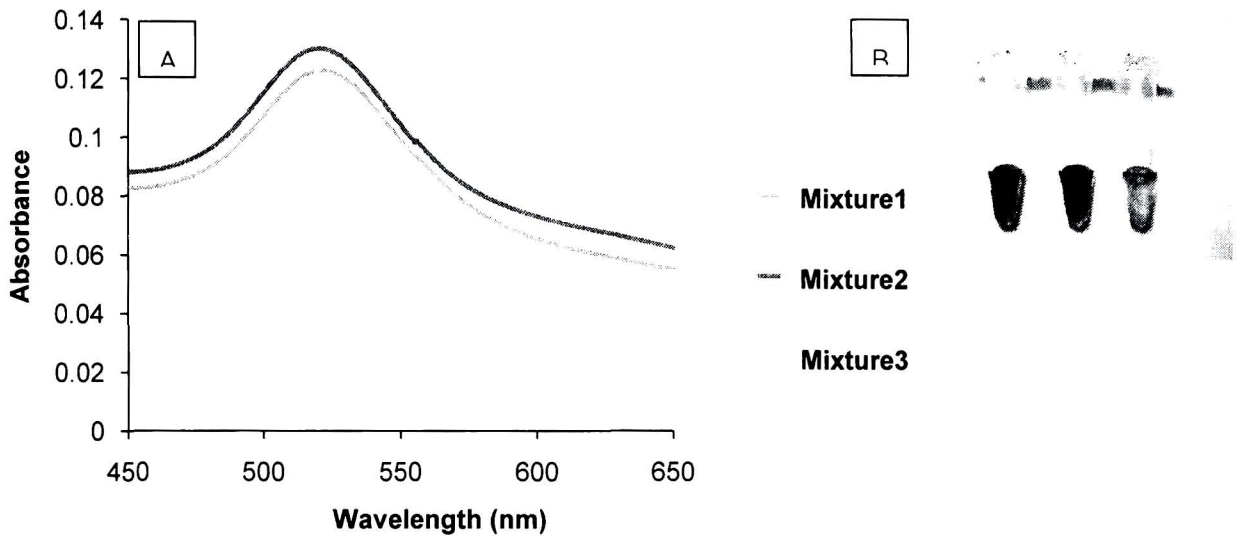


Figure 3.20 Comparison of effect of mixture1-3 on the aggregation of AuNPs. (A) The UV-vis spectra and (B) the colour changing of unmodified AuNPs stabilized by 0.3  $\mu\text{L}$  mixture1-3 from left to right, respectively.

## Colorimetric detection of non-complementary DNA, complementary DNA and 1-mismatched complementary DNA

Non-complementary DNA is the mixture between two non-hybridizable ssDNA. It can be absorbed onto the metal nanoparticles and thus stabilizes the MNPs against the aggregation from the induction of ionic salts. Solutions with adequate quantities of non-complementary DNA prevent aggregation, whereas solutions with complementary DNA (dsDNA) do not affect the aggregation. The comparison between non-complementary DNA and complementary DNA stabilized metal nanoparticles was shown in figure 3.21

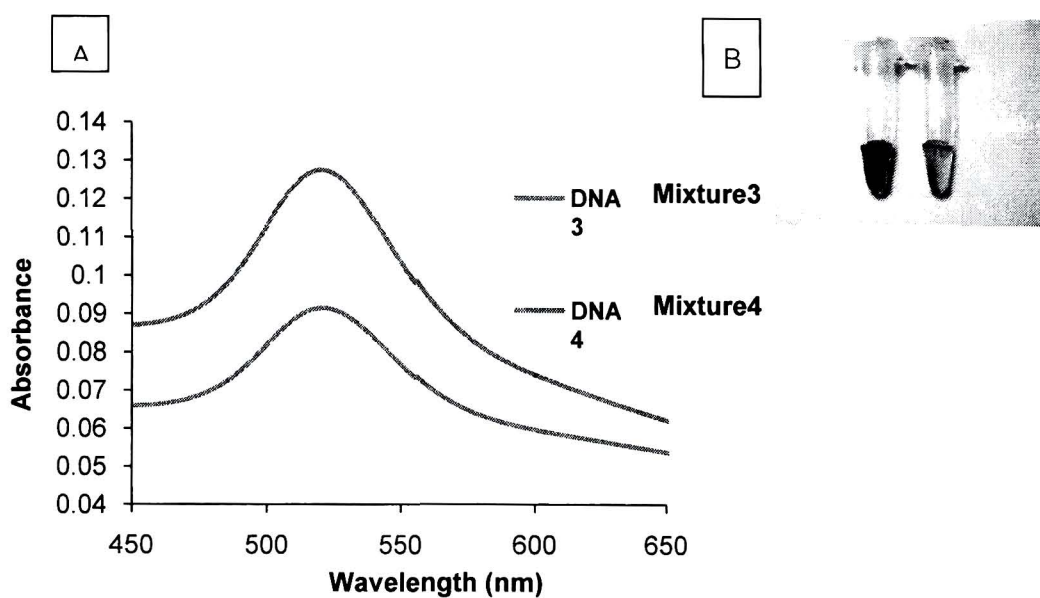
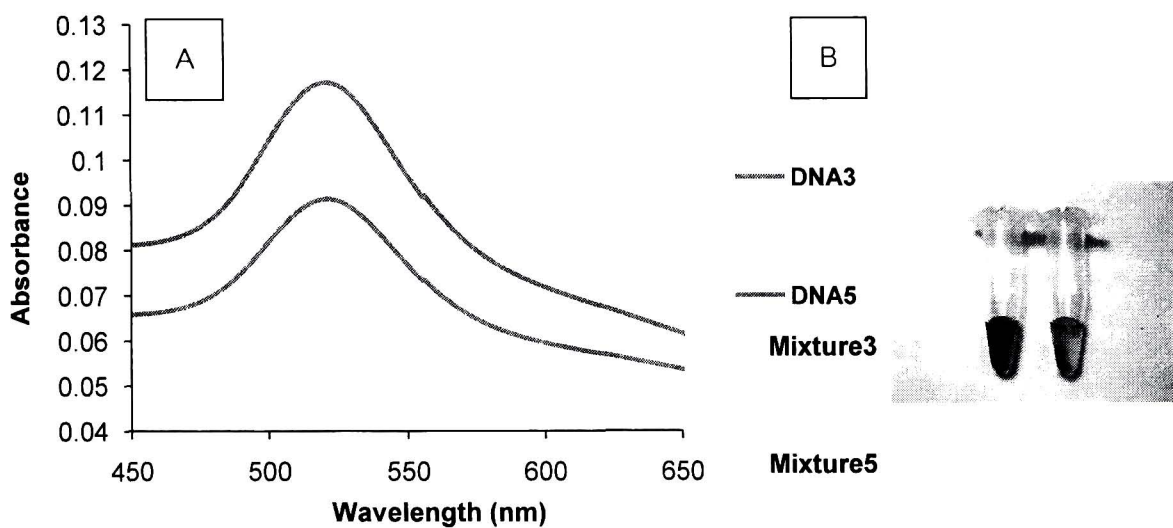


Figure 3.21 Comparison between non-complementary DNA (mixture4) and complementary DNA (mixture3) on DNA stabilization. (A) The UV-vis spectra and (B) the colour changing of unmodified AuNPs stabilized by mixture4 (left eppendorf) and mixture3 (right eppendorf).

Typically, 1-mismatched complementary DNA containing a few base pairs always has lower melting temperature than a perfect complementary DNA for 6-7 °C. Thus, a solution of 1-mismatched complementary DNA contains higher number of ssDNA than those in a perfect matched DNA. As a consequence, 1-mismatched complementary DNA is a better stabilizer for metal nanoparticles than a perfect matched DNA but not as a non- complementary DNA. The comparison between 1-mismatched complementary DNA and complementary DNA stabilized metal nanoparticles was shown in figure 3.22



**Figure 3.22** Comparison between 1-mismatched complementary DNA (mixture5) and complementary DNA (mixture3) stabilized AuNPs. (A) The UV-vis spectra and (B) the colour changing of unmodified AuNPs stabilized by mixture5 (left eppendorf) and mixture3 (right eppendorf).

### **3.5 Optimization of influencing parameters for fabrication of gold nanoparticle-based nucleic acid lateral flow strip test**

The basic principle of AuNPs-based NALF detection system involves the design of thiol-modified specific oligonucleotide probes on AuNPs. If there are complementary targets that can form sandwich hybridization with both thiolated probes on AuNPs and another target-specific probes on test line of the NALF test strip, the functionalized-AuNPs will accumulate at the test line revealing a distinct red color. Previous study reported the utilization of NALF to detect human genomic DNA samples without PCR amplification. Their research group found that the AuNPs based-NALF assay on a test strip had enabled naked eye detection of the target DNA with a very high sensitivity.

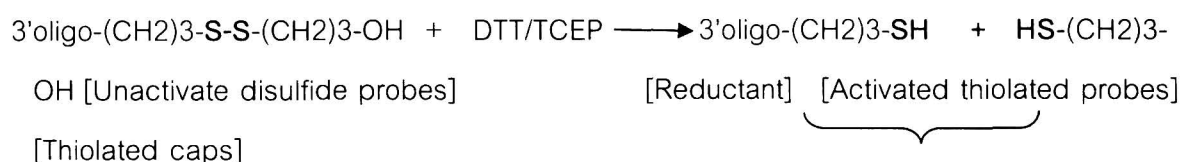
Nonetheless, sensitivity and specificity of the test strip depend on the target-probe hybridization process. The stringency of a buffer system is one of the key determinants of the test result. Changes in ionic concentration in the buffer system can cause AuNPs aggregations and non-specific binding of the nucleic acids. Here in this study, we aimed to improve the processes of AuNPs- thiolated DNA probes conjugation

#### **3.5.1 Effect of reductants on conjugation efficiency**

Results from Table 3.1 indicate that all of the DTT-treated groups had % probe loss lower than those from the TCEP-treated groups. Although the use of TCEP has many advantages, our study revealed that DTT- treated groups have higher conjugation efficiency. The purification of DTT-treated probes with the NAP-5 column removes the thiolated protecting caps which may otherwise compete with the activated thiolated probes for the covalent adsorption on the AuNPs surface as shown below.

Experimental conditions				Results	
Amount of thiolated probes* (nmole)	100 ppm AuNPs (μl)	Type of reductants	Sonication	% Probe loss	Average half-life** (min) (n =2)
1.6	400	DTT	Yes	86.72	16
1.6	400	DTT	No	84.80	8.75
1.6	400	TCEP	Yes	97.45	11.25
1.6	400	TCEP	No	98.08	7.5
0.8	200	-	Yes	68.80	N/A
0.8	200	-	No	70.59	7.5

**Table 3.1.** Experimental protocols studying the effects of reductants and sonication on the conjugation of thiolated probes and AuNPs. (\* The thiolated probes used in this experiment step is probe#1., \*\* Half-life : The time duration taken for half of complete AuNPs aggregation)



“Competitive absorption on Au

### 3.5.2 Effect of sonication on conjugation efficiency

The stability of the conjugated probes was studied by using DTT as a deconjugating agent. Different conjugated probe samples were treated with DTT and incubated at 40°C throughout the experiment. A small portion of each sample was taken out every 5 min and analyzed for an increase in absorbance at 675 nm. Since an increase in the agglomeration of AuNPs will shift the maximum absorbance wavelength from 520 nm to the range between 600-700 nm, the absorbance at 675 nm was chosen as a reference in this study. The measured absorbance at 675 nm was then plotted against time as shown in the deconjugation profile of Fig.3.23. From the deconjugation profile, the initial rise in absorbance is due to the increased aggregation of AuNPs after which the absorbance decreases when the aggregated AuNPs precipitate leaving a relatively more transparent solution. The extent of stability was compared from the half-life values of each group. From the results shown in Table 3.1 and Fig. 3.23., half-lives of the sonication groups (16 and 11.25 min for DTT and TCEP-treated groups respectively) were higher than those of the non-sonication groups (8.75 and 7.5 min for DTT and TCEP-treated groups respectively). This indicates that the sonication increases the stability of the conjugation process. As described in previous work, the sonication reduces undesirable electrostatic force and physical adsorption from bases of thiolated probes on AuNPs surface, which will decrease the sensitivity of the system. When there is less adsorption of the base groups of the probes, more area of AuNPs is available for a stronger covalent adsorption with the thiolated groups of the probes. Such covalent adsorption is more stable than electrostatic force and physical adsorption so it is more desirable

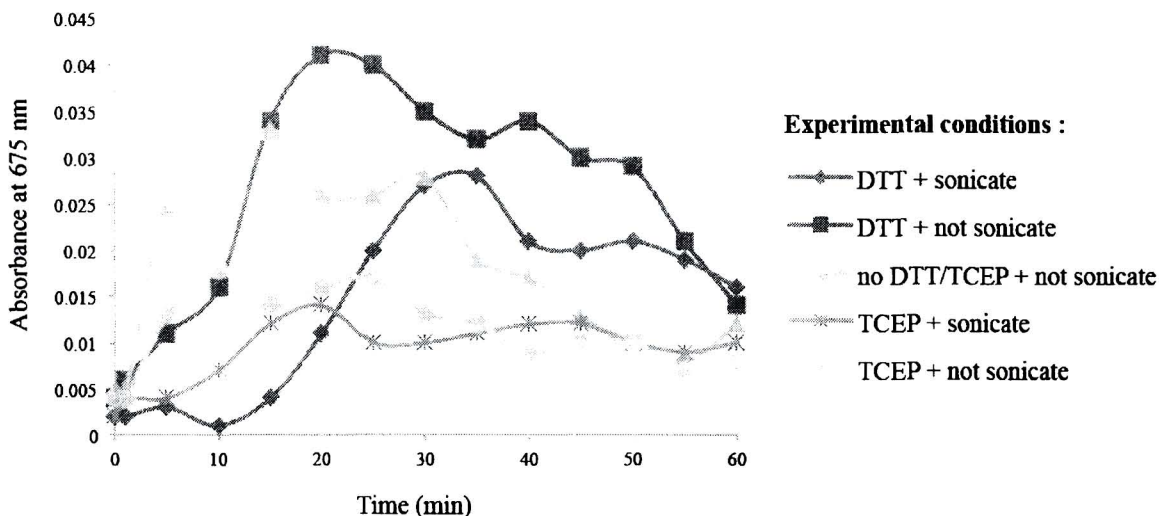


Figure 3.23 Deconjugation profile after DTT treatment on the conjugates.

### 3.5.3 Validation of thiolated probe quantity

The conjugated gold colloid was dispersed in 10 mM phosphate buffer and 150 nM NaCl as the final buffer. After adding DTT to conjugates at 40 °C, the 0.1 and 0.3 nmole samples suddenly turned from red to purple (Table 3.2 and Fig. 3.24). This suggests that these 2 conditions had too few thiolated probes to reach a proper AuNPs stability. Centrifugation of AuNPs was later performed for detecting free thiolated probes in supernatant. The % probe loss was calculated as in Table 3.2. Results showed that the % probe loss were in accordance with amount of thiolated probes used in this study. Moreover, amount of conjugated probes on AuNPs surface are very similar among the 0.3, 0.5, 0.8 nmole samples, whereas the changes of AuNPs color seen by naked eye was observed at 0.3 nmole (Fig. 3.24 (A)). Therefore, this experiment indicates that the optimal quantity for thiolated probe conjugation on AuNPs (20-25-nm size) is approximately 0.5-0.8 nmole.

Experimental conditions			Results		
Amount of thiolated probes* (nmole)	Type of reductants	Sonication	% Probe loss	Amount of conjugated probes on AuNPs (ng/ $\mu$ l)	Color after DTT added
1.0	DTT	Yes	83.05	6.18 $\pm$ 1.17	Red
0.8	DTT	Yes	89.48	4.35 $\pm$ 0.30	Red
0.5	DTT	Yes	76.52	4.68 $\pm$ 0.40	Red
0.3	DTT	Yes	71.43	4.64 $\pm$ 0.31	Purple
0.1	DTT	Yes	45.26	2.76 $\pm$ 0.19	Purple

Table 3. 2. Effect of amount of thiolated probes on AuNPs conjugation.

(\* The thiolated probes used in this experiment is probe#1.)

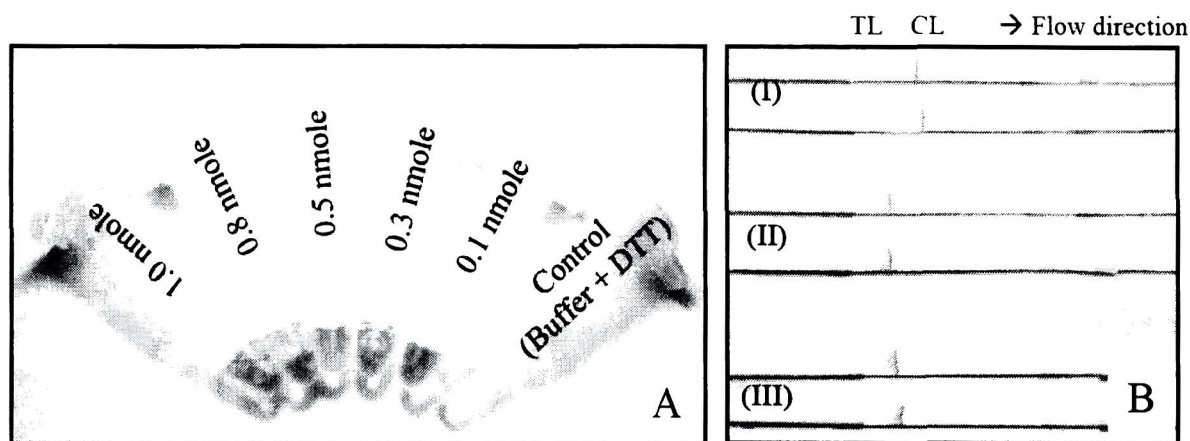


Figure 3.24 (A) The color changes of conjugates after adding DTT. (B) Positive results of lateral flow strip test with DNA targets at (I) 125 fmole, (II) 12.5 nmole and (III) 1.25 fmole (TL = Test line, CL = Control line).

### 3.5.4. Detection of synthetic DNA targets with lateral flow strip test

We used another set of probes (probe#2, 3 and 4) to fabricate the lateral flow test strips as the method described in Mao *et al.* (2009). Synthetic DNA targets at different concentrations were tested on lateral flow platform in order to evaluate the sensitivity of detection limit. The outcome revealed that these test strips could detect the DNA target as low as 1.25 fmole (Fig. 3.24 (B)). To our knowledge, using our modified protocol results in the highest sensitivity of DNA detection by lateral flow test.

## Conclusions

In summary, although TCEP has many advantages over DTT, DTT treatment combined with gel filtration column to remove the thiolated protecting caps is more effective than TCEP treatment in the thiolated probe-AuNPs functionalization. This work showed that the sonication promotes conjugation stability by enhancing the covalent bond formation of thiol moiety and AuNPs surface. The initial amount of thiolated probes used is also critical to obtain the conjugation stability. Finally, we applied this conjugation protocol to construct lateral flow strip tests, results revealed that as low as 1.25 fmole of DNA target is detectable by naked eye detection

### 3.6. Preparation, modification, and testing of antibody-conjugated AuNPs

#### 3.6.1 Optimal amount of antibody to cover and stabilize gold nanoparticles

This project expects that majority part of surface area of gold nanoparticles should be covered by antibody protein. This expectation is aimed to get highest detecting sensitivity and diminish the possibility of unspecific binding that can take place by protein-free area on gold nanoparticles surface. Optimal amount also optimize usage of antibody to be the most effective amount.

Antibody protein has been found to be able to replace citrate around gold nanoparticles and make the nanoparticles to survive in ionic strength solution. Hence, different concentrations of antibody were electrostatically bind to gold nanoparticles surface. After binding, each gold nanoparticles colloids were tested by adding of 10% NaCl. If antibody protein can cover major area of the nanoparticles – which means gold nanoparticles are stabilized by antibody protein instead of citrate, ionic strength solution will not affect to stabilization of gold nanoparticles and the colloid will remain its ruby-red color.

For this project, antibody of *Leptospira pomona* was employed and the result in following part was assumed to be applicable with this antibody only. The antibody was serial diluted in DI H<sub>2</sub>O to have following concentration: 1:2 – 1:10 – 1:50 – 1:100 – 1:500 – 1:1000 volume by volume .

- Raw data

The gold nanoparticles which were admixed with antibody solutions that have concentration equal to 1:2 and 1:10 remain their bright red color while the gold nanoparticles which were blended with lower concentration of antibody (1:50, 1:100, 1:500, 1:1000) were aggregated and their color were altered.

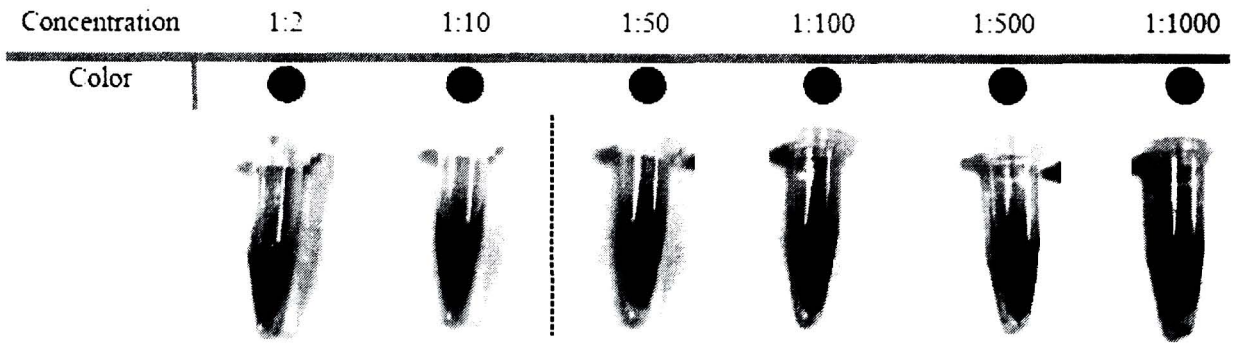


Figure 3.25 Result of stabilization of gold nanoparticles that are conjugated with different concentration of antibody to find the most optimistic concentration to be used in following step. The first two tubes remain their color while the others tubes are agglomerating.

- Discussion

The color of gold nanoparticles changed significantly since 1:50 diluted antibody solution, lower concentration (1:50, 1:100, 1:500, 1:1000) led to less nanoparticles surface covering while higher concentration solutions (1:2, 1:10) did cover the gold nanoparticles very well.

Hence, 1:10 diluted antibody is seem to be the most optimistic amount which satisfy both experimental way and economical way.



❖ Functionalization, tester preparation, and detecting process

Common procedure of antibody-conjugated gold nanoparticles preparation is illustrated in Fig 3.27 which consists of eight major steps (A1-A8) while Figure represents preparation process of antigen on nitrocellulose membrane (B1-B7) including usage of antibody-conjugated gold nanoparticles to detect antigen on the membrane ( )

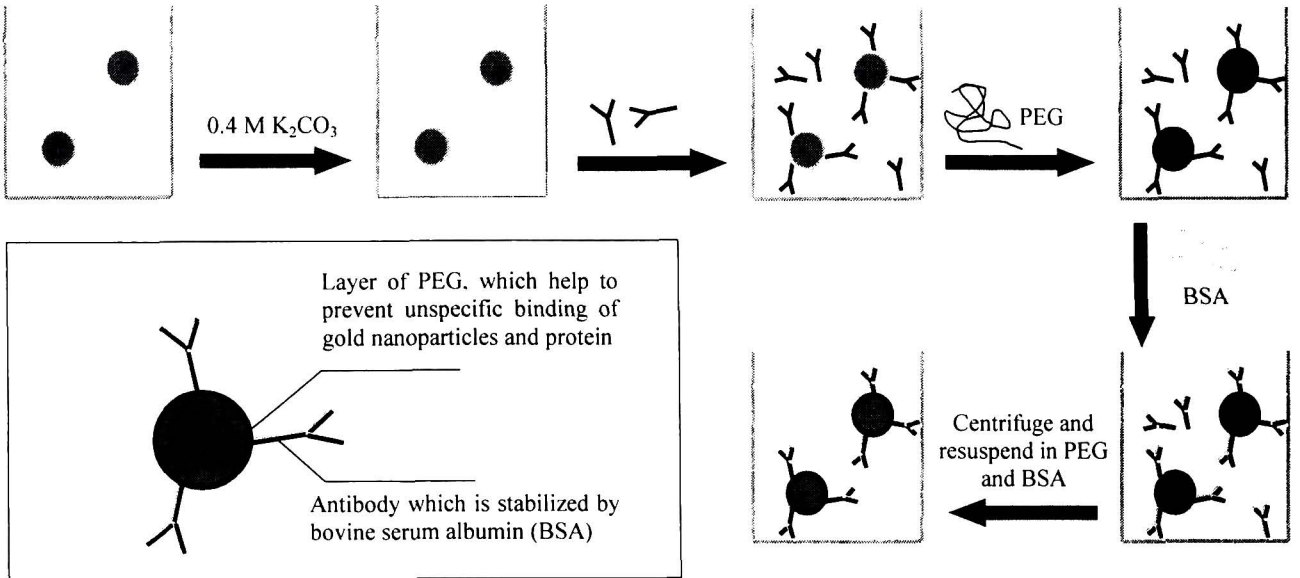


Figure 3.26 - Schematic representation of functionalization procedure by conjugating antibody onto gold nanoparticles.

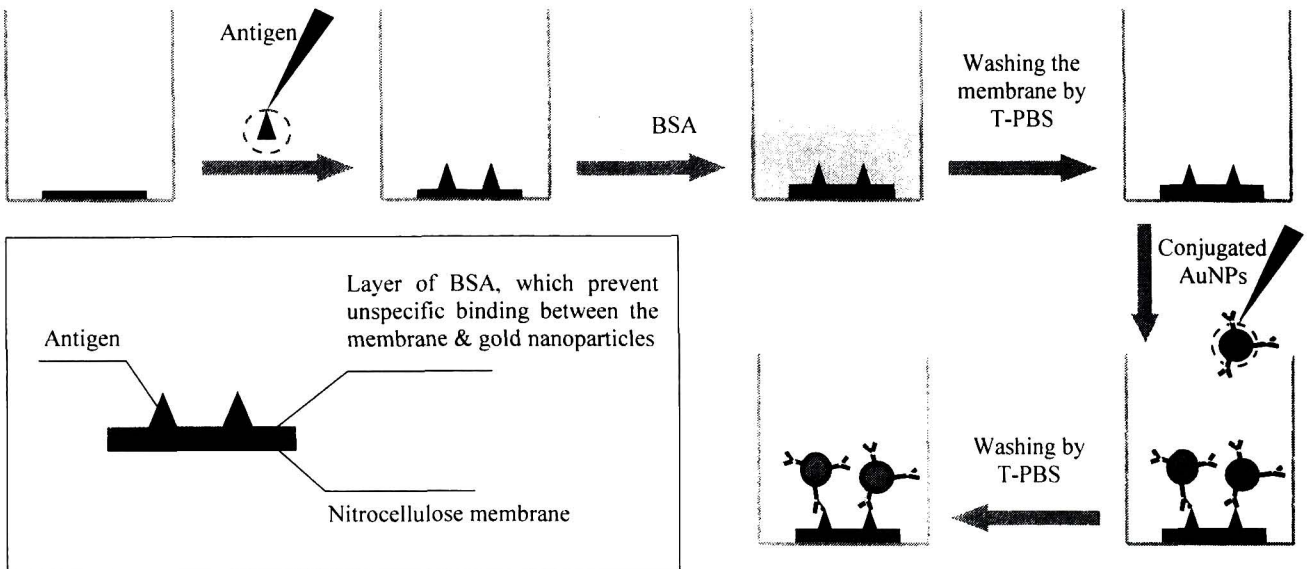


Figure 3.27 - Schematic representation of placing antigen onto nitrocellulose membrane and membrane blocking process. Include the process of antigen detection using *L. pomona* antibody-conjugated gold nanoparticles and washing process.

### 3.6.2 General detection of antigen by antibody-conjugated gold nanoparticles

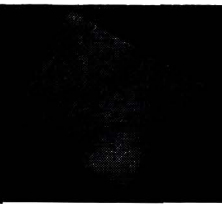
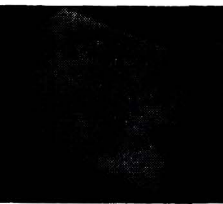
Antibody-conjugated gold nanoparticles has been examined to be a sensitive and easy method for detect specific antigen protein. In this project, antibody of *Leptospira pomona* was employed to be conjugated on gold nanoparticles surface using the procedure described above.

In the meantime, nitrocellulose membrane was cut into 5 pieces and put into well number A1-A5. The antibodies which had been dropped on those nitrocellulose membranes were *Leptospira pomona*, *Leptospira pyrogenase*, *staphylococcus aureus*, *Escherichia coli*, and 1X PBS in well A1-A5 respectively.

In this general detection, all conditions were set for the most convenient aspect. Thus, we set the antibody-gold nanoparticles incubation time to be 15 minutes, added PEG and BSA in PBS to mix with conjugated gold nanoparticles before centrifuge. The solution was centrifuged in 4°C using speed and time stated above. The experiment was carried out with antigens that had concentration equal to  $10^5$  cells per 1 mL agitated without diluted. The membranes were blocked by BSA in PBS and the length of sensing period was 30 minutes precisely.

- Raw data

When *L. pomona* antibody-conjugated gold nanoparticles was impregnation in the well that contained antigen-bound nitrocellulose membrane, antibody on gold nanoparticles surface would spontaneously bind to antigen protein that conserved some matching part. For here, the red dot of gold nanoparticles noticeably appeared on nitrocellulose membrane in well A1 which *Leptospira pomona* antigen was dropped. Meanwhile, vague signals of gold nanoparticles were observable in well A2 and A3. However, there was no signal can be detected in well A4 and A5.

Antigen	<i>L. pomona</i>	<i>L. pyrogenase</i>	<i>S. aureus</i>	<i>E. coli</i>	1x PBS
signal					

**Figure 3.28** Result of general antigen detection using *L. pomona* antibody-conjugated gold nanoparticles. This experiment was expected to express the fundamental capability of functionalized gold nanoparticles for biosensing application. The signal was fully detectable in the case that type of antigen and antibody was matching. However, some signals from cross-reaction of antigen-antibody could happen due to the fact that bacteria themselves also conserve some interference sequences of protein. [Remark: the figures are tuned for better contrast while the experimental result is still unaffected.]

- Discussion

The ability of *L. pomona* antibody-conjugated gold nanoparticles was satisfied because it can detect the existence of *Leptospira pomona* antigen as we can see from Figure 3.29. However, the incident of signals in well number A2 and A3 which are not *L. pomona* are concluded to be the problem of antigen-antibody interaction. Due to the fact that antigen proteins of *Leptospira pyrogenase* which is being in the same genus with *Leptospira pomona* also contain some interfering sequences. Meanwhile, the major outer membrane protein sequences of *Leptospira pomona* which contains specific antigens are also matching with some sequences of *Staphylococcus aureus*' proteins as Pubmed's BLAST software can examine out in Figure 3.29. Both two cases are called cross-reaction of antigen-antibody protein which is drawback of this technique, thus, more purified antibody should be employed if better result is expected.

```

GenBank: AAT45362.1

major outer membrane protein [Leptospira noguchii serovar Pomona]

>gi|48526308|gb|AAT45362.1| major outer membrane protein [Leptospira noguchii
serovar Pomona]
MKKLSILAISVALFASITACGAFGGLPSLKSSFVLSEDIIPGNETIVKILLPYGSVINYGYVVKPGQAPD
GLVDGNKKAYLYVWIPAVIAEMGVRMISPTGEIGEIPGDGLVSDAFKAATPEEKSMPHWFDTWIRVERM
SAIMPDQIAKAAKAKPVQKLDLDDDDGDDTYKEERHNKYNSLTRIKIPNPPKSFDDLKNIIDTKLLVRGLY
RISFTTYKPGEVKGSFVASVGLLFPFGIPGVSPLIHSNPEELQKQAIAAEESLKKAASDATK

```

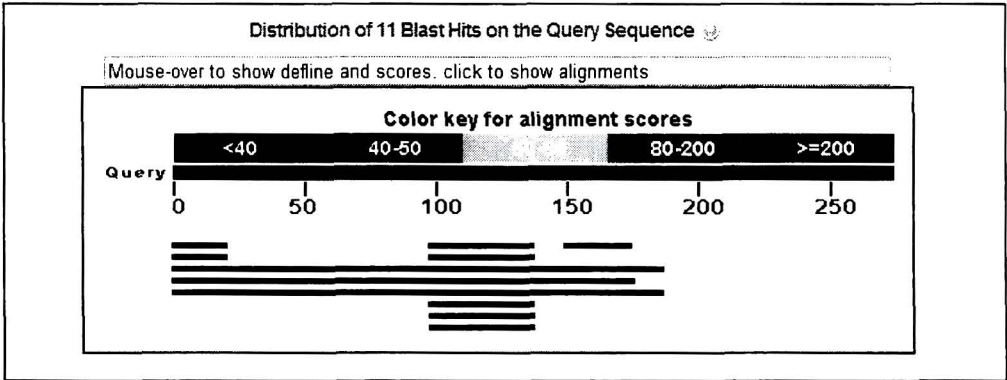


**Figure 3.29** - (Upper) Sequences of major outer membrane proteins of bacteria *Leptospira pomona*. The format of sequences is FASTA that is brought from National Center of Biotechnology Information (NCBI)'s Pubmed protein databases (cited on 13<sup>th</sup> April 2009). (Lower) schematic diagram of blast hits between major outer membrane protein sequences and proteins presenting in bacteria *Staphylococcus aureus*. The black line is showing the estimated region that protein sequences are interfering.

For the last two wells, antibody-conjugated gold nanoparticles cannot detect any signals due to the facts that *Escherichia coli* antigen proteins and 1X PBS which is the negative control is unmatched with our biosensing material.

Selectivity of our *L. pomona* antibody-conjugated gold nanoparticles is satisfied because it can detect existence of *Leptospira pomona* antigen and express out the distinguishable signal from the others unexpected signal which is the result from cross-reaction.

From this general detection, although gold nanoparticles can function well to diagnose the presence of antigen, sensitivity of detection still low. Hence, the following experiments were anticipated to get better sensitivity of detection and the most appropriate conditions were examined.

### 3.6.3 Effect of antibody-gold nanoparticles incubation time

The functionalization of gold nanoparticles by attaching of antibody protein is electrostatic reaction which is a reversible reaction that antibody can attach and detach alternatively all the time. To complete the attachment, it requires just enough length of time for conjugation process. For here, we examined the effect of incubation time that affect to the final signal intensity of gold nanoparticles to detect antigen. Four tubes of conjugating gold nanoparticles were incubated for 15 minutes, 30 minutes, 60 minutes, and 120 minutes while continuously mixed.

- Raw data

It was observed that all conjugated gold nanoparticles which antibody incubation time was different did not show any obvious physical dissimilarity. Their colors after preparation were comparable as shown in Figure . The sensitivity of all gold nanoparticles was also the same in intensity which is visible for human naked eyes observation, Figure 3.30.

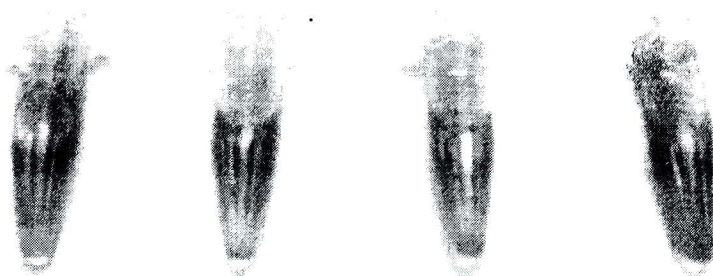


Figure 3.30 - final *L. pomona* antibody-conjugated gold nanoparticles. They had different antibody incubation time as (Left to Right) 15 mins. 30 mins. 60 mins. and 120 mins. respectively.

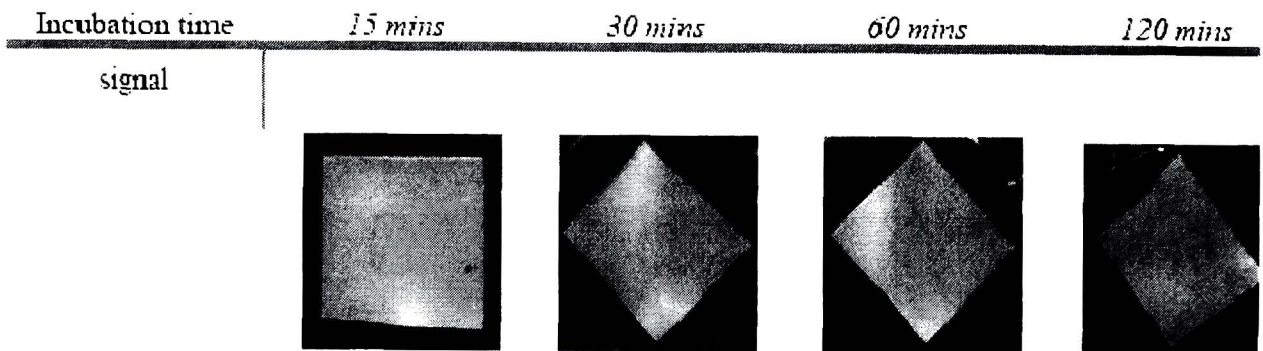


Figure 3.31 Effect of antibody incubation time upon the final signal intensity in antigen detection proces

- Discussion

As the result showed that there is no significant difference in signal intensity, it means 15 minutes is enough length of time for antibody protein to attach onto surface of gold nanoparticles. Longer time after 15 minutes which the attachment has already reached its limitation is not necessary. It also tells that different incubation time does not affect to stability of antibody-conjugated gold nanoparticles as their color remain the same for all tubes.

### 3.6.4 Effect of centrifuge temperature

Protein is the biomaterial that is very sensitive to the environment. Basically, proteins have to be kept in low temperature to prevent them from denature. This fact is also applicable to our project, since we expected that all steps of antibody-conjugated gold nanoparticles preparation process should be conducted in cold temperature especially during step of centrifuge which antibody protein have to face with crucial conditions and easily to be denatured. Two tubes of antibody-conjugated gold nanoparticles probe were prepared in the same manner except temperature that was set for centrifuge, the probe which was centrifuged at 4 degree centigrade (4°C) was used to detect antigen on raw A while the other was centrifuged at room temperature and was used with antigen on raw B.

- Raw data

There were observable signals in well A1-A3 which 4°C centrifuged gold nanoparticles probe was employed to detect antigen while no signal appeared in all wells on raw B, which room temperature probe was used whether there is the nitrocellulose membrane that contained antigen of *L. pomona* in well B1.

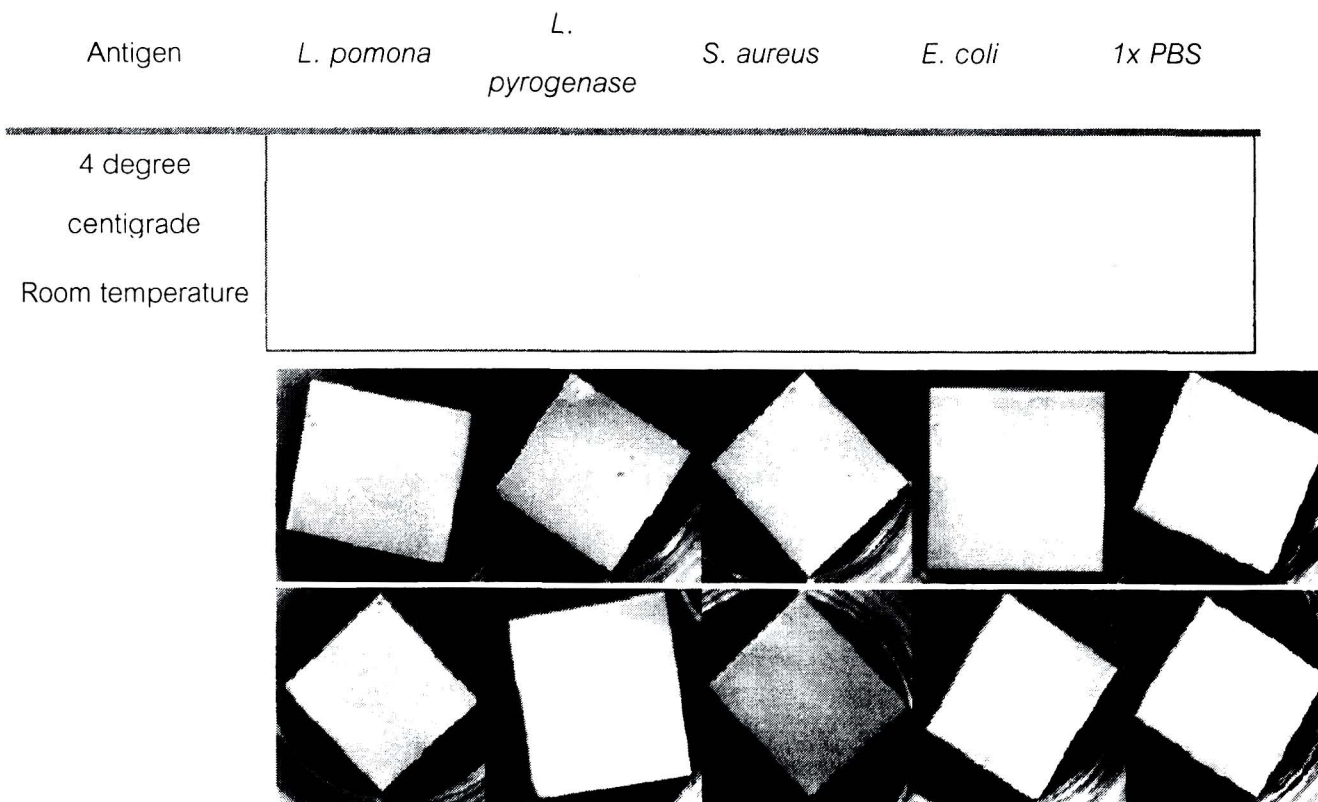


**Figure 3.32** – Effect of centrifuge temperature upon the final detecting signal of *L. pomona* antibody-conjugated gold nanoparticles probe. It seems like antibody had detached from surface of gold nanoparticles during room temperature centrifuge which make the gold nanoparticles lose their sensing capability

- Discussion

Centrifuge temperature seems to affect the functional ability of conjugated gold nanoparticles significantly. As the signals from the probe that were centrifuged in room temperature were very low in intensity and were not visible for naked eyes which should be result of detachment of antibody during centrifuge. While the signals from 4°C centrifuged probe still expressed satisfied detectable signal of presenting of *L. pomona* antigen. Thus, centrifuge has to be conducted in cold conditions to maintain attachment of antibody and maintain sensitivity of the gold nanoparticles probe.

### 3.6.5 Effect of existence of PEG in conjugated gold nanoparticles solution

Polyethylene glycol or PEG is the polymer that has enough affinity to spontaneously attach on gold nanoparticles surface. It has higher affinity than citrate and normally used as gold nanoparticles polymeric stabilizer in many cases. In this project, PEG was used as blocking substance to cover on antibody-free region on gold nanoparticles surface and prevent unspecific binding between gold nanoparticles and antigen protein during sensing. However, it shows some possibility that PEG can diminish signal intensity - that means it can reduce sensitivity of our *L. pomona* antibody-conjugated gold nanoparticles probe. Two antibody-conjugated gold nanoparticles are prepared with and without PEG and tested with the tester membrane of all antigen types that we have. The conjugated gold nanoparticles with PEG were tested with antigen on raw A while PEG-free probe was tested on raw B.

- Raw data

There were noticeable signals of gold nanoparticles in well A1 and B1 which contained antigen of *L. pomona*. The signal intensity in well B1 was also significantly bold when compared to signal in well A1. However, antibody-conjugated gold nanoparticles probe with PEG on raw A showed up signal only in well A1-A3 but the PEG-free probe on raw B generated signal in well B1-B4. The result is shown in Figure 3.33.

Antigen	<i>L. pomona</i>	<i>L. pyrogenase</i>	<i>S. aureus</i>	<i>E. coli</i>	1x PBS
Probe with PEG					
Probe without PEG					

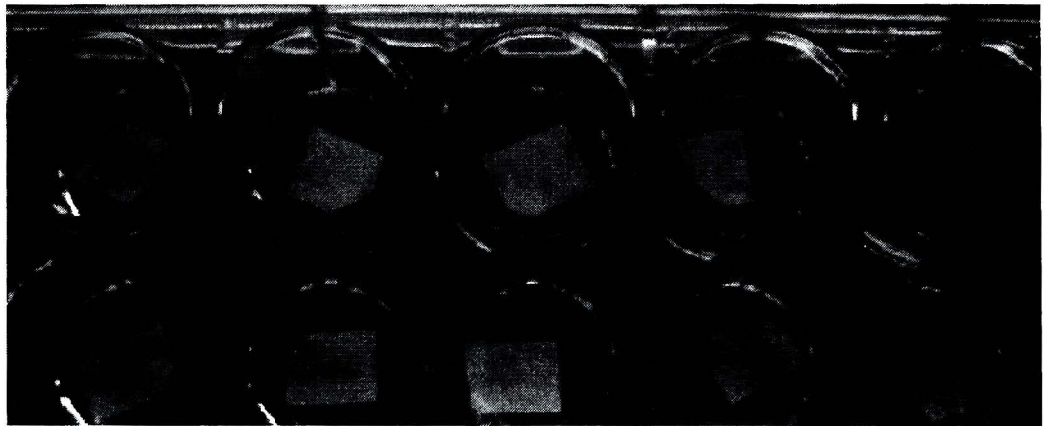


**Figure 3.33** – Effect of PEG upon the final signal intensity when conjugated gold nanoparticles probes were used to detect antigen. (Upper) The sensing signal of *L. pomona* antibody-conjugated gold nanoparticles with PEG (Lower) Sensing signal of PEG-free conjugated gold nanoparticles.

#### - Discussion

Polyethylene glycol is obviously affect to sensitivity of gold nanoparticles probe, it can act as spacer or mask that reduce the binding of antigen-antibody and make the strength of sensing signal to be lower than actual. However, when PEG is lack, some region on gold nanoparticles surface are naked and make them to be able to unspecifically bind to antigen protein.

### 3.6.6 Effect of concentration of antigen protein and minimal amount of antigen to be detectable

The amount of antigen presenting on nitrocellulose membrane is directly related to the observable signals. For here, minimal amount of antigen to be detectable by our prepared antibody-conjugated gold nanoparticles was examined. The concentrations of stock solution of our antigens are  $10^8$  *Leptospira pomona* cells per 1 milliliter of sterile DI H<sub>2</sub>O agitated well by sonicator machine. We took those stock solutions and diluted them by 1X, 0.1X, 0.01X, and 0.001X in sterile DI H<sub>2</sub>O. The diluted antigen solutions were assumed to be equivalent to  $10^8$ ,  $10^7$ ,  $10^6$ , and  $10^5$  bacterial cells per 1 mL of sterile DI H<sub>2</sub>O.

#### - Raw data

There was just one visible signal of gold nanoparticles that appeared only in well A1. The signal was relatively low but still observable by naked eyes. Meanwhile, there was no signal occurred in the others wells, said, well B1, C1, and D1 which contained 0.1X, 0.01X, and 0.001X diluted antigen as shown in Figure 3.34.

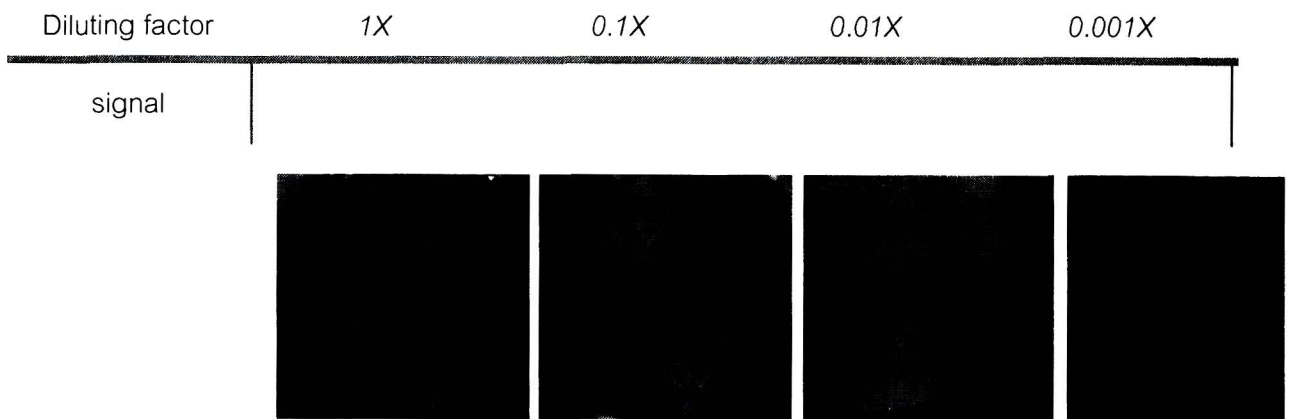


**Figure 3.34** – Effect of concentration of antigen to the sensitivity of *L. pomona* antibody-conjugated gold nanoparticles and experiment to examine the minimal amount of antigen that our gold nanoparticles can detect. From picture, we can detect the antigen with 1X diluting factor which equivalent to  $10^8$  bacterial cells per 1 mL and this is the minimal amount that can be detected by our probe.

#### - Discussion

From this experiment, we can know the lowest limit of our antibody-conjugated gold nanoparticles probe which is  $10^8$  agitated bacterial cells per 1 milliliter. Hence, lower

concentration of antigen that this minimal point is undetectable by our conjugated gold nanoparticles. However, this limitation also depends on types and quality of antigen and antibody which were employed here. With antibody that has higher quality can express higher sensitivity and lower concentration of antigen may be diagnosable.

### **3.6.7 Effect of blocking agent upon the detecting signal by antibody-conjugated gold nanoparticles**

Blocking agent plays an important role in blotting diagnostic process. Because blocking process is the step that can prevent unspecific binding between proteins on the probe, such as antibody protein of the conjugated gold nanoparticles, with the mismatch region of antigen protein or even some part of nitrocellulose membrane. Generally, milk (e.g. skim milk) which contains protein named casein is used as blocking agent in conventional blotting process such as western blotting. However, from previous study about nanoparticles, bovine serum albumin (BSA) which is holding protein called albumin was normally employed as blocking agent instead of milk. Albumin will cover antigen-free region on the membrane and inhibit agglutination between antibody protein and the membrane which will generate wrong positive signal. The different between using BSA and milk as blocking agent was studied by prepare two rows of antigens which were blocked differently. Membranes on row A were blocked by BSA while the membranes on row B were blocked by Carnation® milk. Both of them were tested by a set of antibody-conjugated gold nanoparticles.

#### **- Raw data**

Detectable signal on well A1 was obvious for human eyes while weak signals on the well A2 and A3 were fairly noticeable. There was also a very weak signal took place on the membrane in well B1. However, the others well had no sign of signal.

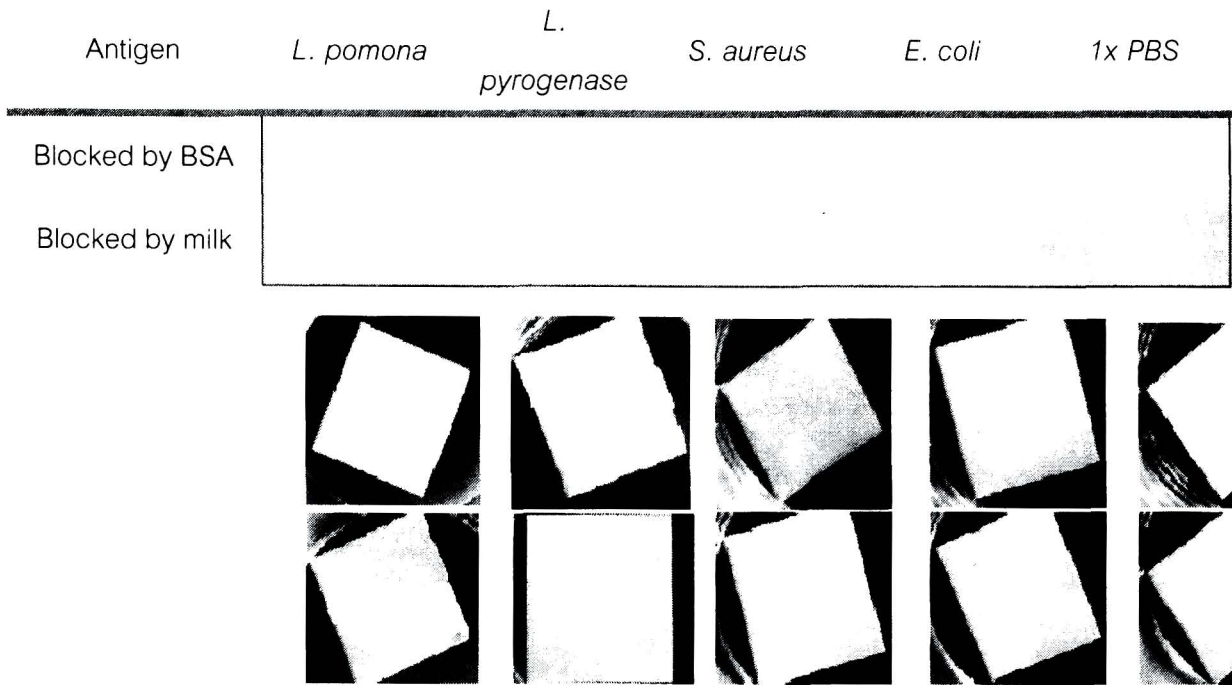


Figure 3.35 -- Effect of blocking agent to the function of *L. pomona* antibody-conjugated gold nanoparticles. (Upper) Membranes were blocked by bovine serum albumin and the signals appeared on well A1-A3. (Lower) Membranes were blocked by milk. Very low signal which nearly invisible for human naked eyes appeared on B1.

- Discussion

There was a weak signal appeared on the membrane in well B1 while no signal was observable in well B2-B5. These may be concluded that milk is a better blocking agent than BSA in the sense of selectivity; it may deduce the signals caused by weak bonding of cross-reaction very well. However, for the sake of sensitivity, BSA is better blocking agent because its signal is easier to be observed during screening diagnosis.

### 3.6.8 Effect of impregnation time for conjugated gold nanoparticles to detect existence of antigen

Antibody-conjugated gold nanoparticles are spontaneously bound onto specific antigen that can match very well with the antibody on the nanoparticles. When the nanoparticles probe was impregnated with antigen-dropped nitrocellulose membrane by antigen-antibody interaction would be strongly influenced by the length of time. Actually, the effect of impregnation time was studied in the following experiment which the same set of antibody-conjugated gold nanoparticles and antigen-bound nitrocellulose membrane were used. The difference among each wells were the length of time for impregnation; 15 minutes, 30 minutes, 60 minutes, 90 minutes, and 120 minutes were set up for the wells number A1-A5 respectively. The antibody used in this case was *L. pomona* while the antigen dropped onto the membrane was also the cell fragment of bacteria *L. pomona* only.

- Raw data

There were weak signals showed up on the membrane in well A1 and A2 which impregnation time were 15 minutes and 30 minutes correspondingly. The signals became obviously by human naked eyes since the well A3-A5 which impregnation equal to 60 minutes and longer. Figure shows the signal from different impregnation time for conjugated gold nanoparticles to detect antigen.

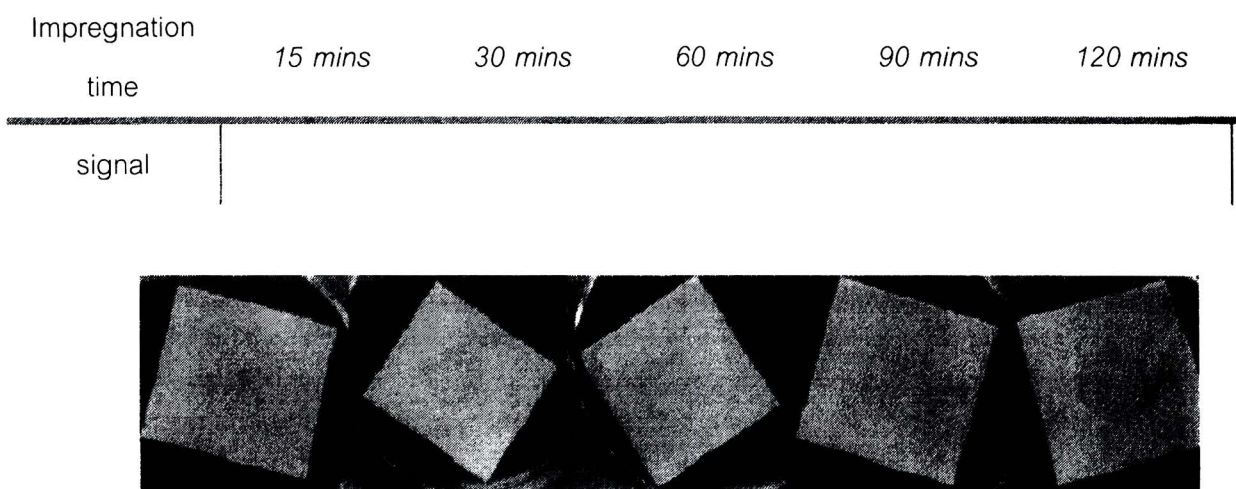


Figure 3.36 Effect of *L. pomona* antibody-conjugated gold nanoparticles sensing time upon the signal intensity that can be observed by human naked eyes.

- Discussion

From the result, it is clearly that antigen-antibody binding and deposition of gold nanoparticles onto specific nitrocellulose membrane was utilized by impregnation time. The signal was strong enough to observe when impregnation time is equal or longer than one hour or 60 minutes which can be assumed as the most appropriate length of time. We also can conclude that all results from variation of the others factors reported above which is normally keep in detecting for 30 minutes will show stronger signal intensity or higher sensitivity if it was incubated for longer time (e.g. 60 minutes).



### 3.6.9 Silver-enhancing to improve signal intensity of conjugated gold nanoparticles

● Using of silver to enhance the signal received from detection by gold nanoparticles probe.

The schematic procedure of silver enhancement is illustrated in Figure 3.37 below.

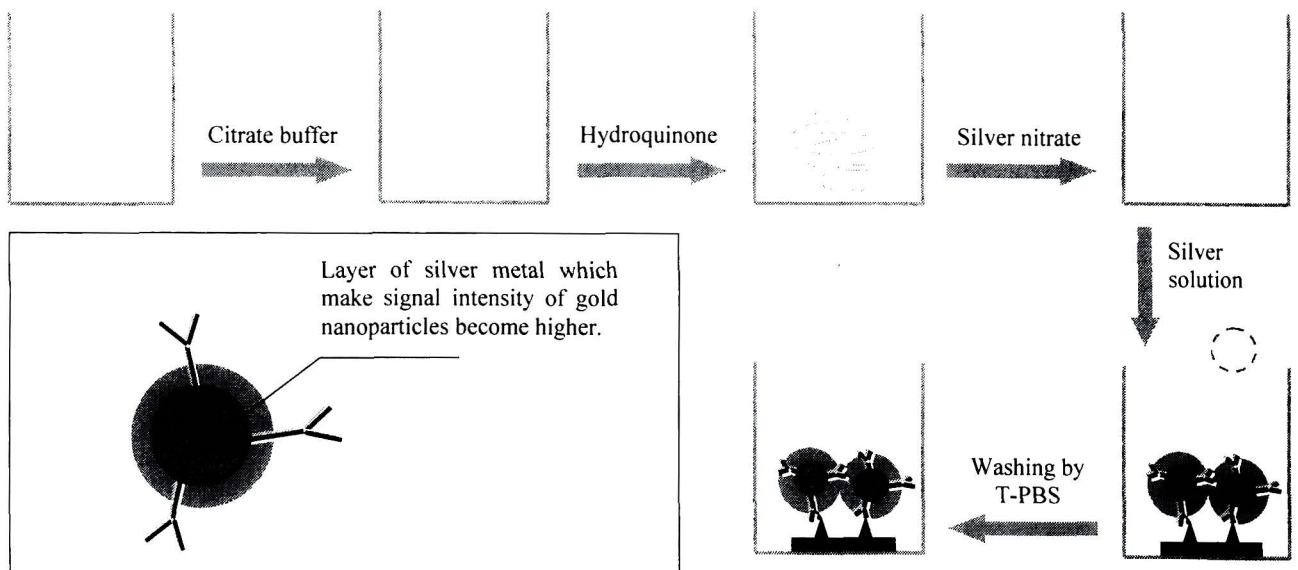


Figure 3.37 schematic representation of silver enhancing process

Effect of silver enhance upon the signal from different impregnation time of gold nanoparticles probe

This experiment is the continue part from the experiment labeled '*Length of impregnation time for conjugated gold nanoparticles to detect existence of antigen*'. The silver solution was freshly prepared and added into the well A1-A5. The incubation time for silver solution to enhance the signal of gold nanoparticles is 10 minutes long for this experiment in dark. However, the signal was increased sophisticatedly after the membranes with silver solution had already been washed out were exposed to light for 5 minutes more.

- Raw data

From previous experiment, the signals from conjugated gold nanoparticles were obviously noticeable since the well A3-A5 which impregnation times were 60 minutes, 90 minutes, and 120 minutes. Meanwhile, the signals in well A1 and A2 which were 15 minutes and 30 minutes impregnation were almost invisible. After enhanced by silver solution, all signal intensities in every well were increased. The signals in well A1 and A2 become easily detectable while the signals in others wells become more apparent.

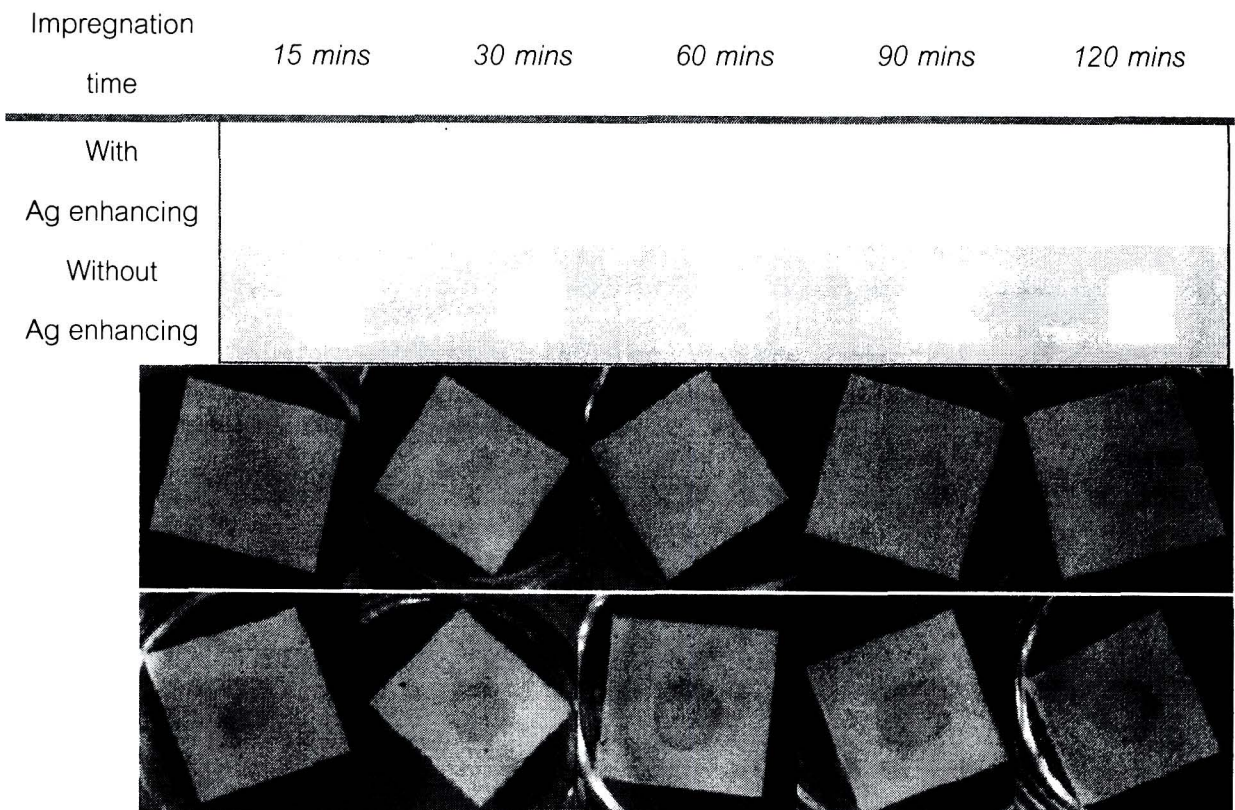


Figure 3.38 - Effect of silver enhance upon the signal from different detection time of *L. pomona* antibody-conjugated gold nanoparticles to detect antigen from bacteria *Leptospira pomona*. (Upper) From left to right, the detected signal from gold nanoparticles for 15, 30, 60, and 120 mins, respectively without silver enhancement.

## Discussion

Silver enhancement seems to have the ability to increase the signal intensity from detection by *L. pomona* antibody-conjugated gold nanoparticles. Generally, biosensing materials are aimed to diagnose rapidly with shorter than one hour long, so, the gold nanoparticles probe itself cannot meet this condition. However, silver enhanced gold nanoparticles can show up a clear visible signal within 15 minutes of gold nanoparticles impregnation with enhancing process that takes just another 15 minutes more. Thus, the signal can be received within 30 minutes for the whole process of detection and it is more appropriate for screening diagnosis purpose

## 3.7 Detection of Leptospira in urine using anti-Leptospira-coated gold nanoparticles

### 3.7.1 Preparation of antibody-coated gold nanoparticles

Preparation of antibody-coated gold nanoparticles *Leptospira interrogans* serovar Bratislava was used in this study because it is a representative of the most common serogroup reported in Thailand. According to the report of Zhao et al, the pH of gold nanoparticle suspension was adjusted to 9.0 prior to antibody coating. In this study, optimum pH of gold solution was also determined (data not shown) and gold particle suspension adjusted to pH 9.0 was used for antibody coating in further experiments. Various amounts of antibodies were tested for gold particle coating. Anti-*Leptospira* antibody was diluted to 1:2, 1:10, 1:20 and 1:100. Diluted antibodies were incubated with gold nanoparticles for 15 min at room temperature before adding 100 ml of 10% NaCl. Gold nanoparticles coupled with antibody dilution 1:2, 1:10 and 1:20 (Fig. 3.39, Tubes # 1, 2 and 3, respectively) gave red color solution after NaCl was added whereas the color of gold suspension with antibody dilution 1: 100 (Tube # 4) turned blue. This suggested that the amount of antibody in 1:100- dilution tube was not enough to couple gold particles used. The 1:10 antibody dilution was used in further experiments.

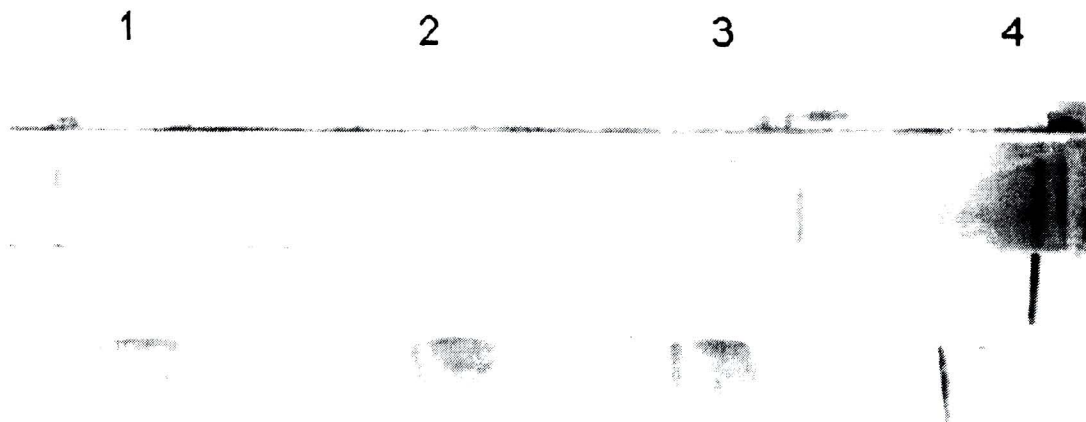


**Figure 3.39** Optimum antibody dilution for preparing antibody-coated gold particles. Gold nanoparticle suspension pH 9.0 was incubated with antibody diluted to 1:2, 1:10, 1:20 or 1:100 as described in Section 2. After adding NaCl solution, the suspension with antibody dilution 1:2, 1:10, 1:20 gave red color (Tubes # 1–3). The blue color of suspension in Tube # 4 indicated that the amount of antibody used was inappropriate.

### 3.7.2 Detection of *Leptospira* in urine using *Leptospira* antibody-coated gold nanoparticles

*Leptospira interrogans* serovar Bratislava was spiked into urine from a normal individual to the final concentrations of 1, 10,  $10^2$ ,  $10^3$ ,  $10^4$ ,  $10^5$ ,  $10^6$ ,  $10^7$  and  $10^8$  leptospire/ml. Two hundred microliters of urine containing various amounts of *Leptospira* was centrifuged and the sediment was resuspended in 20ml of deionized distilled water, pH 9.0 before testing with anti-*Leptospira*-coated gold particles. Agglutination of red gold nanoparticles indicates the positive result. No agglutination was observed when antibody-coated gold particles were tested with urine without *Leptospira* added or when uncoated gold particles were tested with urine containing *Leptospira* (data not shown). Agglutination of gold particles was seen when urine containing 10,  $10^2$ ,  $10^3$ ,  $10^4$ ,  $10^5$ ,  $10^6$ ,  $10^7$  and  $10^8$  leptospire/ml was tested (Fig. 3.40, Tubes # 2–9). There was no agglutination in tube containing one leptospire/ml (Tube # 1). These data suggested that the sensitivity of detection was 10 leptospire/ml. Since only 200ml of urine was used, our assay could detect *Leptospira* even there was as few as 2 leptospire presence.

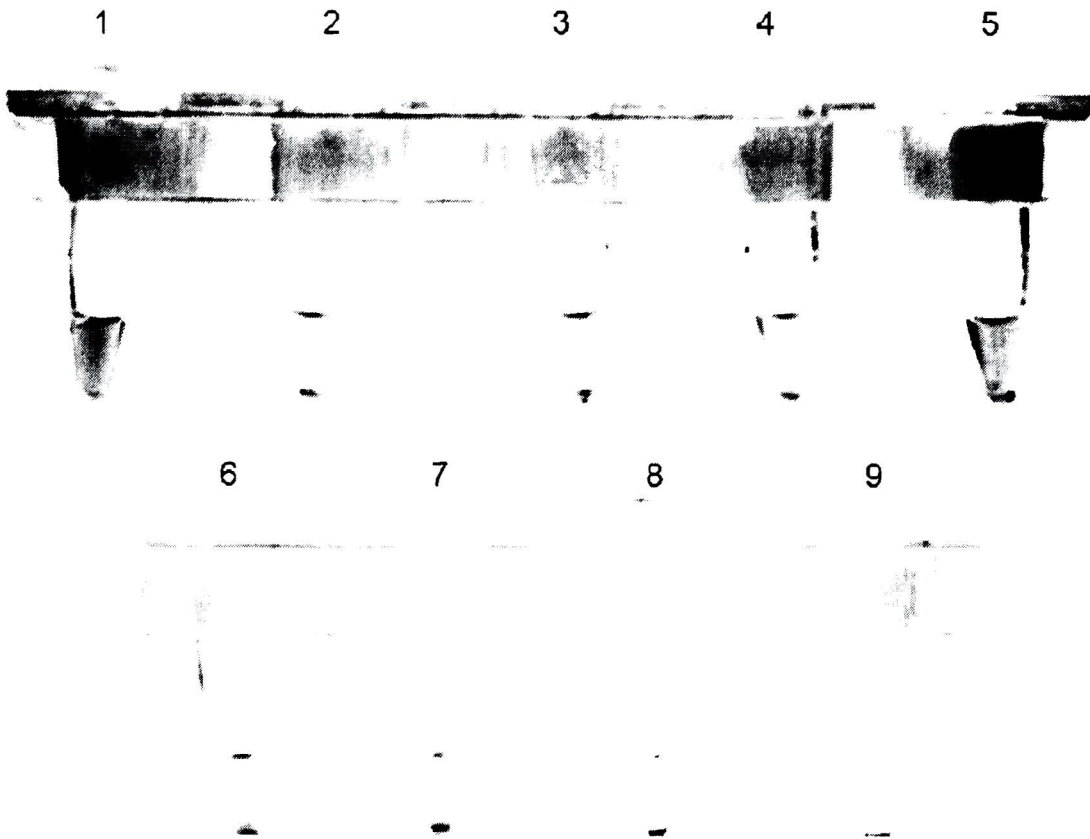


**Figure 3.40** Detection of *Leptospira* in urine. Urine containing 1, 10, 102, 103, 104, 105, 106, 107 and 108 leptospires/ml (Tubes # 1-9, respectively) was centrifuged and the sediment was resuspended in deionized distilled water. The suspension was then mixed with antibody-coated gold particles as described in Section 2. Agglutination of gold particles could be observed in Tubes # 2-9.

### 3.7.3 Specificity of anti-Leptospira-coated gold particles

Leptospira antibody-coated nanoparticles were also tested with other organisms commonly found in urine. As shown in Fig. 3.41, no agglutination was observed when anti-Leptospira-coated particles were tested with *Escherichia coli*, *Klebsiella pneumoniae*, and *Enterococcus faecalis* (Tubes # 2–4, respectively). Tube # 1 was a positive control which urine containing *Leptospira* was tested.

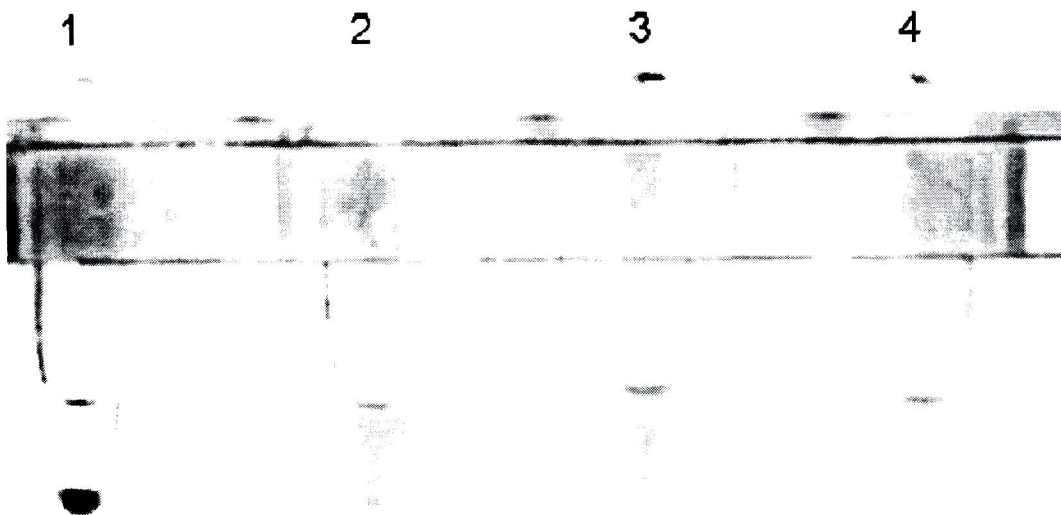


**Figure 3.41** Specificity of *Leptospira*-coated gold nanoparticles. *Leptospira* antibody-coated gold particles were tested with *Escherichia coli*, *Klebsiella pneumoniae*, and *Enterococcus faecalis* (Tubes # 2–4). Tube # 1 contained *Leptospira* which was used as a positive control in this experiment.

#### Discussion

Laboratory diagnosis for Leptospirosis commonly relies on antibody detection. It has been shown that *Leptospira* can be detected in urine before the eighth day of illness [22]. In addition, urine collection from patients is not invasive as blood collection is. *Leptospira* antigen detection in urine has been reported [23]. This method requires special equipment and is not easy to perform. PCR for detection of *Leptospira* in urine samples have also been demonstrated [24,25]. However, the rapid and simple assays should be developed for infectious disease diagnosis so the tests can be performed in any laboratories and the results can be obtained quickly for proper treatment. Our assay could detect *Leptospira* in urine even the amount of *Leptospira* was as few as 2 cells. The assay was inexpensive, simple and easy to perform. The

positive result could be observed immediately to within 15min when urine with  $10^8$ ,  $10^7$ ,  $10^6$ ,  $10^5$ ,  $10^4$ , and  $10^3$  leptospire/ml were tested. Urine containing 102, and 10 leptospire/ml gave positive results within 60min. The antibody-coated particles can be stored at 4 C at least for 2 months without losing the sensitivity of detection (data not shown). Moreover, urine sample can be kept frozen at -20 C if it cannot be processed and tested immediately after collection. In summary, our data demonstrate that gold nanoparticles can be used in the development of a rapid and simple assay for detection of *Leptospira* in urine samples. Further study, such as coupling of gold particles with antibody that can react with all pathogenic *Leptospira* should strengthen the usefulness of this assay.

## Conclusion

In summary, here we established in house citrate-stabilized gold nanoparticles. Our studies showed that these synthesized nanomaterial is capable of using for biomedical application. The DNA-conjugated and antibody-conjugated gold nanoparticles was shown to be practicable biosensing material. In the case of polyclonal antibody which was electrostatically conjugated, the sensitivity was high enough for primary screening diagnosis purpose while the whole process of detection was superior to the others blotting process such as western-blotting or conventional dot-blotting. In this project, many physical and chemical conditions were studied and examined their effect to the capability of antibody-conjugated gold nanoparticles. It was obviously that temperature, existence of polyethylene glycol (PEG), blocking agents, and impregnation time have influent effects to the functions of biosensing material made from gold nanoparticles. In addition, the silver-enhanced process was capable to increase intensity of the signals from gold nanoparticles and to reduce the whole processing time required per a case of detection. We also established an optimized procedure for lateral flow strip test fabrication. This knowledge would be useful a promising template for making a new tool for detection of microorganisms e.g. bacteria causes fever of unknown origin. Further studies to investigate the possibility of employing silver enhancement in the using of gold nanoparticles for *in vitro* infectious disease detection can bring us to the new era of primary screening diagnosis which will make more convenient life for human.

## ข้อเสนอแนะเกี่ยวกับงานวิจัยในชั้นต่อไป

1. งานวิจัยนี้ได้ทำการผลิตอนุภาคทองคำระดับนาโนเมตรซึ่งมีคุณภาพดี เสถียรที่อุณหภูมิห้อง และสามารถนำไปประยุกต์ใช้งานในทางการแพทย์ โดยการนำไปใช้เป็นเครื่องตรวจหาสารชีวโมเลกุล (Biosensor) ได้ทั้งการตรวจหาดีเอ็นเอและโปรตีน พบว่าอนุภาคทองคำระดับนาโนเมตรที่สังเคราะห์ขึ้นมาใหม่เป็นพิษต่อเซลล์มนุษย์ และมีราคาถูกมากกว่ายี่สิบเท่าเมื่อเทียบกับราคาของสินค้าที่มีขายในต่างประเทศ ดังนั้นจึงมีความเป็นไปได้ที่จะสามารถผลิตอนุภาคทองคำระดับนาโนเมตรออกมาเป็นปริมาณจำนวนมาก เพื่อการใช้ในการวิจัย และการประยุกต์ใช้ในเชิงพาณิชย์ต่อไป
2. งานวิจัยนี้ต้องมีความรู้เรื่องปัจจัยทางเคมีและกายภาพในการควบคุมการสร้างอนุภาคทองคำระดับนาโนเมตร รวมทั้งปัจจัยทางกายภาพและทางเคมีที่มีผลต่อการผลิตแผ่นตรวจโรคโดยอาศัยหลักการของ Lateral flow strip test ซึ่งได้ทำการทดสอบแล้วในห้องปฏิบัติการ จึงมีความเป็นไปได้ที่จะสามารถนำความรู้นี้ไปใช้เป็นต้นแบบในการพัฒนาชุดตรวจโรคอื่นๆได้อีกมากมาย ที่อาศัยการตรวจหาดีเอ็นเอและแอนติบอดีของสิ่งส่งตรวจ
3. งานวิจัยค้นพบว่าการใช้อนุภาคเงินระดับนาโนเมตร สามารถเพิ่มความไว (sensitivity) ในการตรวจหาดีเอ็นเอ และ แอนติบอดีของเชื้อก่อโรค ที่ต้องการตรวจได้ โดยจะเสริมความไวในการทำงานของอนุภาคทองคำนาโนเมตร จึงมีความเป็นไปได้และเป็นข้อเสนอแนะให้ใช้อนุภาคเงินนาโนเมตรมาเป็นองค์ประกอบในชุดตรวจโรคอื่นๆที่จะจัดสร้างขึ้นเพื่อให้ใช้เป็นชุดตรวจโรคที่ต้องการ
4. ด้วยประสิทธิภาพของอนุภาคทองคำนาโนเมตรที่สามารถตรวจหาได้ทั้งดีเอ็นเอและโปรตีนที่สนใจ จึงมีความเป็นไปได้ที่จะพัฒนาต่อยอดให้มีการปรับปรุงพื้นผิวของอนุภาคทองคำนาโนเมตรให้สามารถตรวจลูกผสมได้ทั้งดีเอ็นเอและโปรตีน โดยการติดดีเอ็นเอโพรบสายสั้นและแอนติบอดีของแอนติเจนที่สนใจเข้าไปที่ผิวของอนุภาคทองคำนาโนเมตร
5. ในการตรวจหาเชื้อก่อโรคซึ่งในบางกรณีมีจำนวนของดีเอ็นเอและ/หรือแอนติบอดีจำนวนน้อย อาจทำให้เกิดผลลบหลวง (false negative) ได้ในการตรวจสิ่งส่งตรวจที่มี genomic DNA ของมนุษย์ สามารถเพิ่มความจำเพาะ (specificity) และความไว (sensitivity) ของการตรวจนี้ได้โดยการให้ Peptide nucleic acid (PNA) probes แทน DNA probes
6. ต้นแบบชุดตรวจโรคที่ได้นี้ ได้มีการจดสิทธิบัตรแล้ว และอยู่ในระหว่างการขยายผลสู่ภาคอุตสาหกรรม